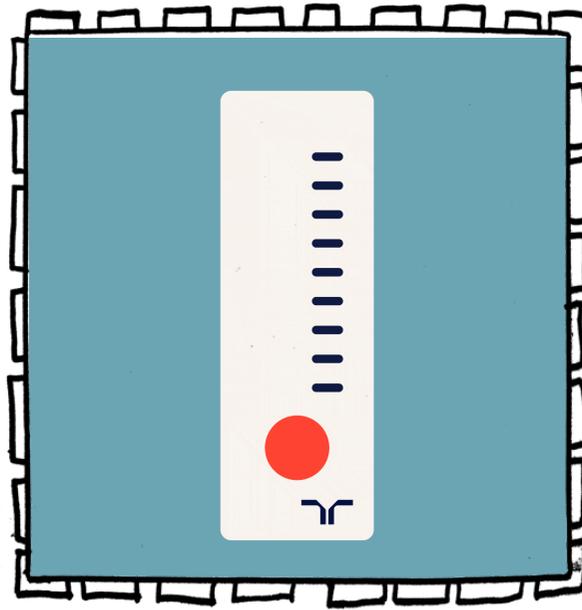# La température

Culture scientifique en L3
Institut Villebon-Charpak, Julien Bobroff
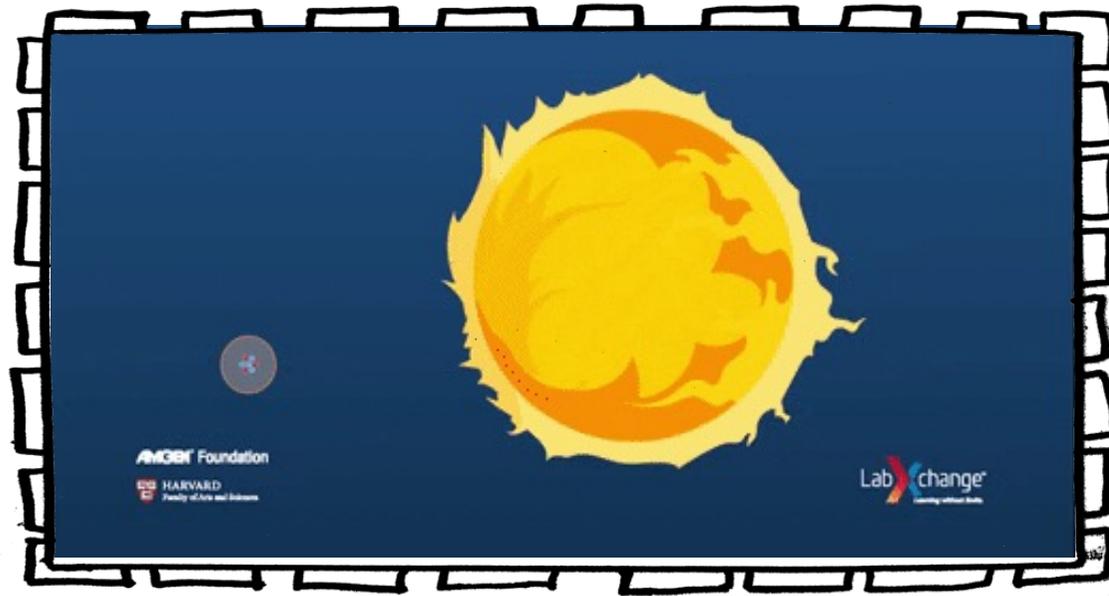
La température

expliquez à un enfant de 10 ans ce que c'est

La température

quelles équations ?

La température

les ordres de grandeur

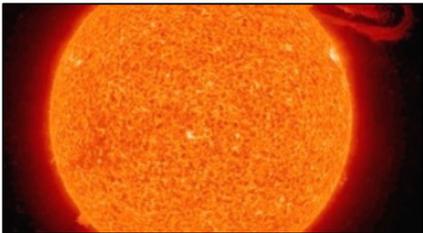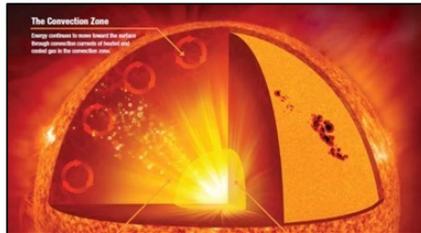# Classez du plus chaud au plus froid (en Kelvin)
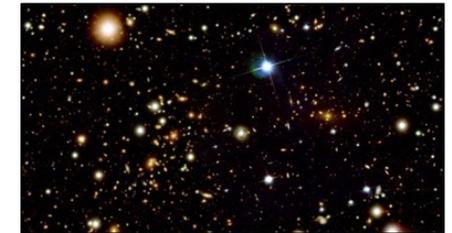

humain

Vostok

azote liquide

helium liquide

surface du soleil

coeur du soleil

bougie

espace
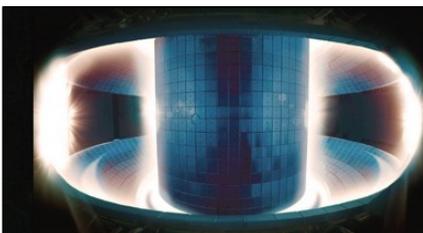
plasma en fusion

moteur de voiture
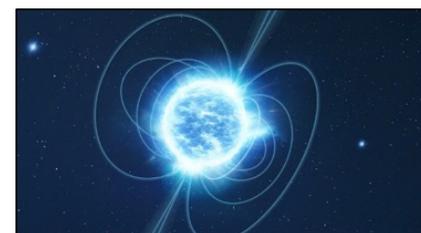
étoile à neutrons
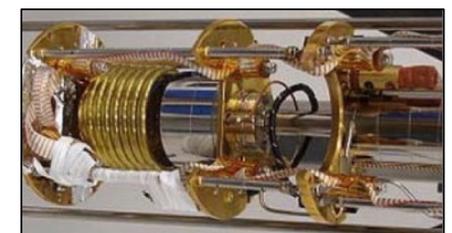
cryostat à dilution

Classez du plus chaud au plus froid (en Kelvin)
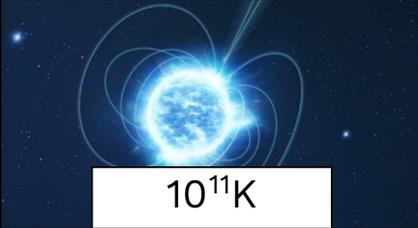
10^{11}K
étoile à neutrons
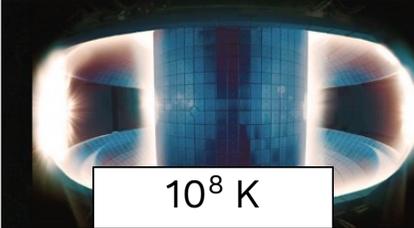
10^8 K
plasma en fusion
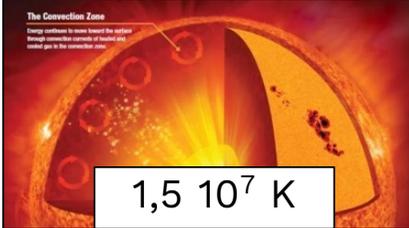
$1,5 \: 10^7$ K
coeur du soleil
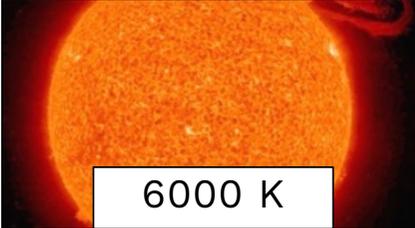
6000 K
surface du soleil

1000 à 2000 K
bougie
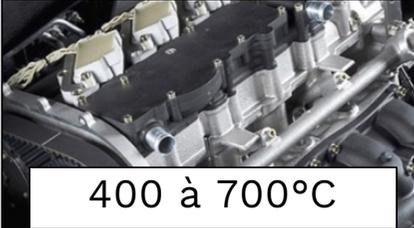
400 à 700°C
moteur de voiture

37°/310K
humain
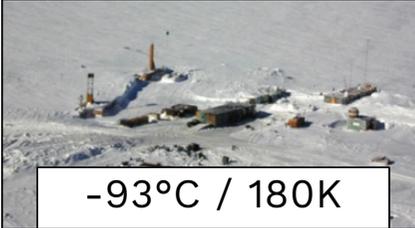
-93°C / 180K
Vostok

-196°C / 77 K
azote liquide
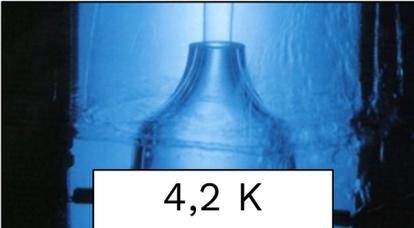
4,2 K
helium liquide
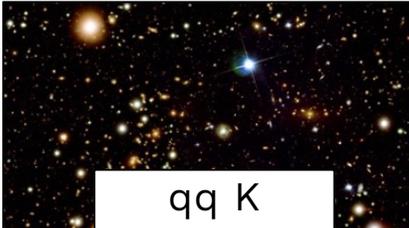
qq K
espace
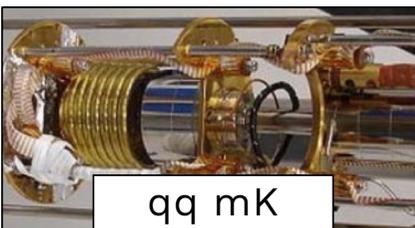
qq mK
cryostat à dilution

Température (Kelvin)

qq K	-196°C / 77 K	1000 à 2000 K		$1,5\ 10^7$ K
espace	azote liquide	bougie		coeur du soleil

10^{-3} 1 100 10 000 10^6

qq mK	4,2 K	37°/310K	6000 K
cryostat à dilution	helium liquide	humain	surface du soleil
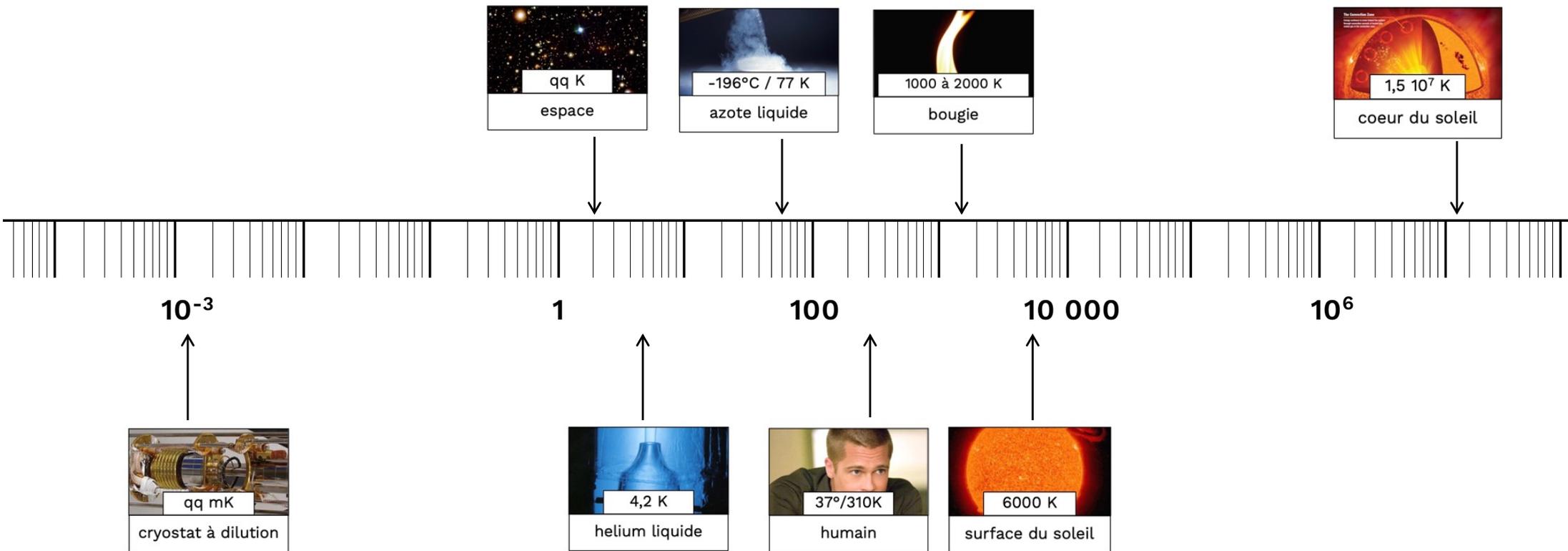
La température

mesure et contrôle

comment refroidir ?

en utilisant un liquide froid

comment refroidir ?
La liquéfaction des gaz
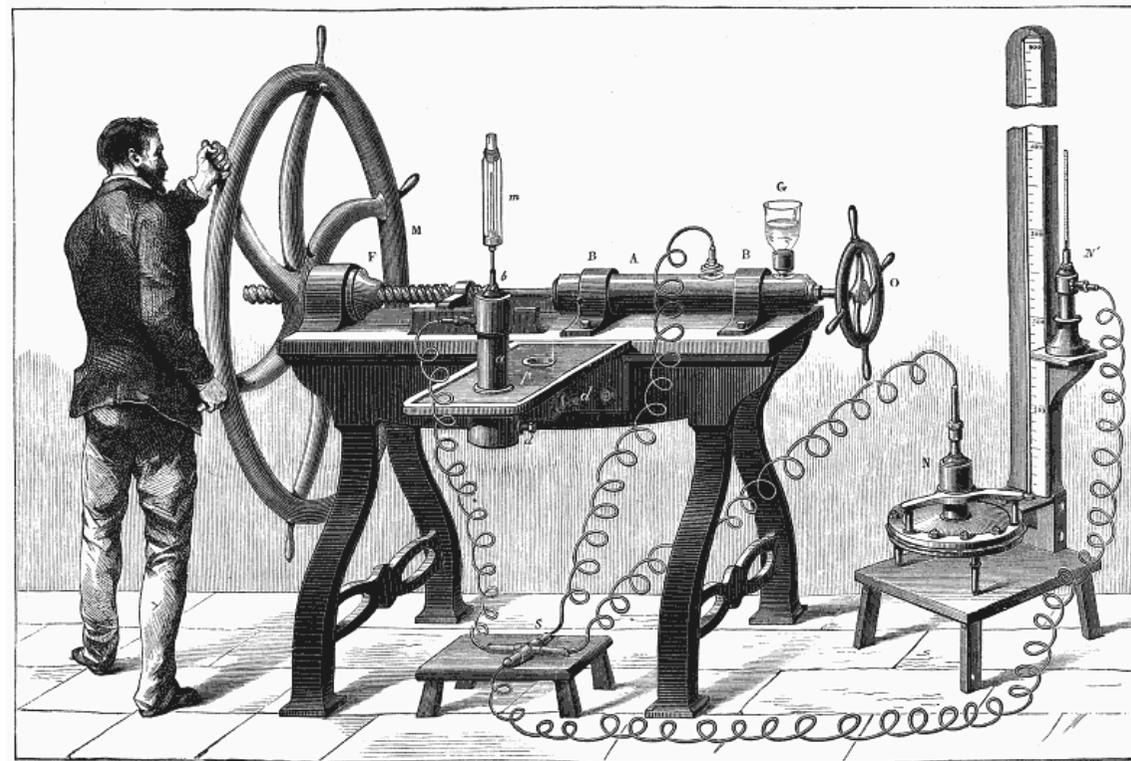
Fig. 1.—CAILLETET'S APPARATUS FOR LIQUEFYING GASES.

1877 : Cailletet et Pictet liquéfient l'oxygène (-183 °C) et l'azote (-195°C)

comment refroidir ?

La liquéfaction des gaz

1898 J. Dewar: liquéfaction de l'hydrogène (-250 °C)

comment refroidir ?
La liquéfaction des gaz
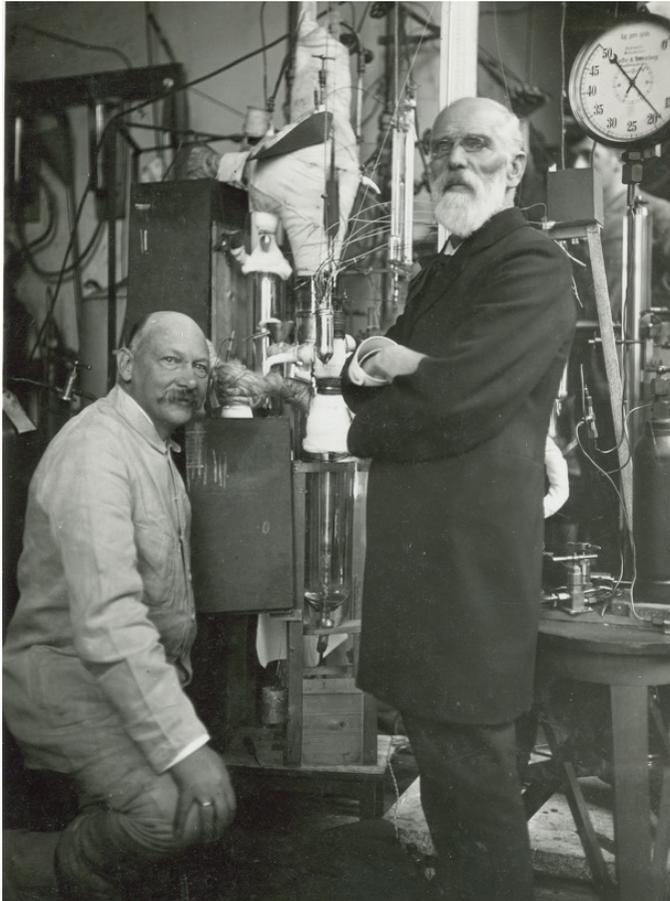
1908 K. Onnes:
liquéfaction de l'hélium (-269 °C)

l'hélium
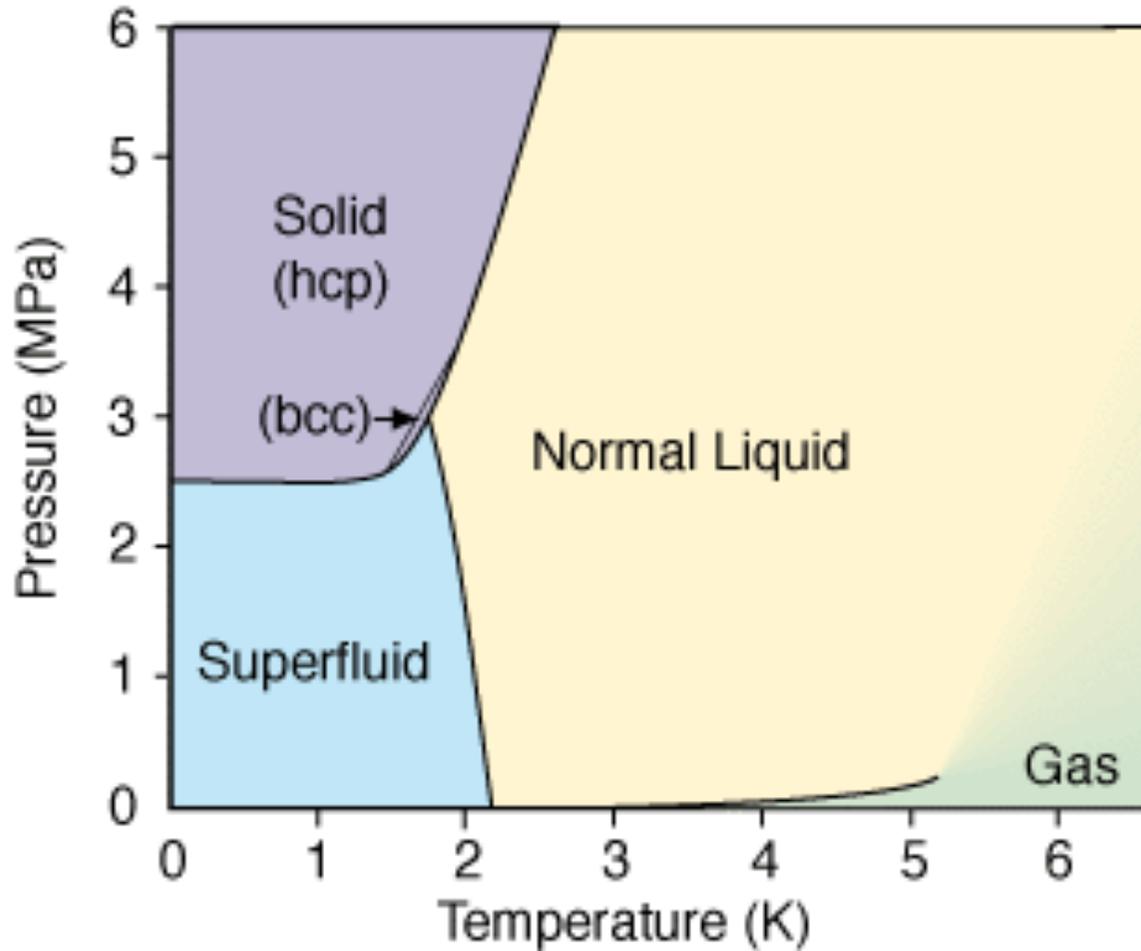
- liquide sous 4,2K

- superfluide sous 2,17K

- solide seulement sous pression

l'hélium superfluide

superfluidité : la viscosité devient nulle

les atomes forment soudain un condensat quantique.
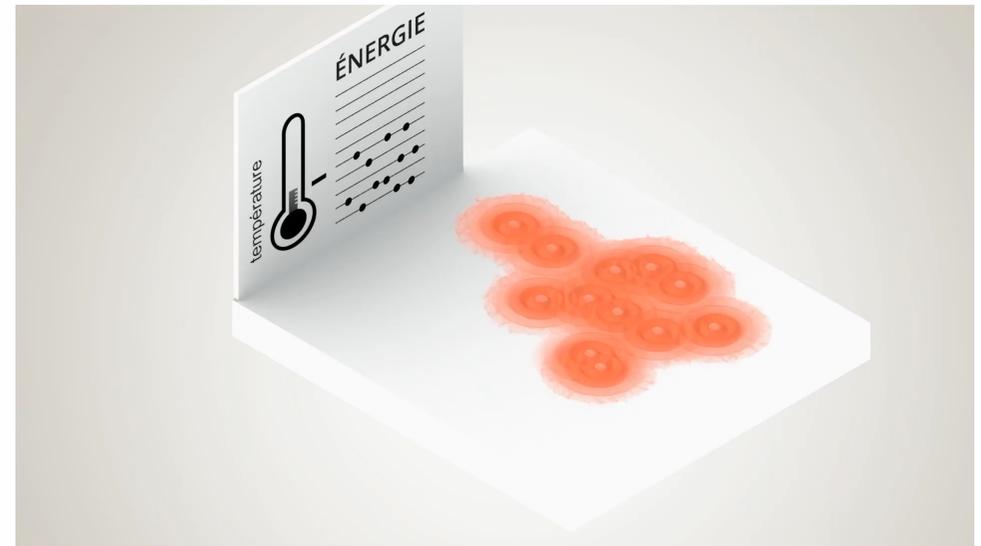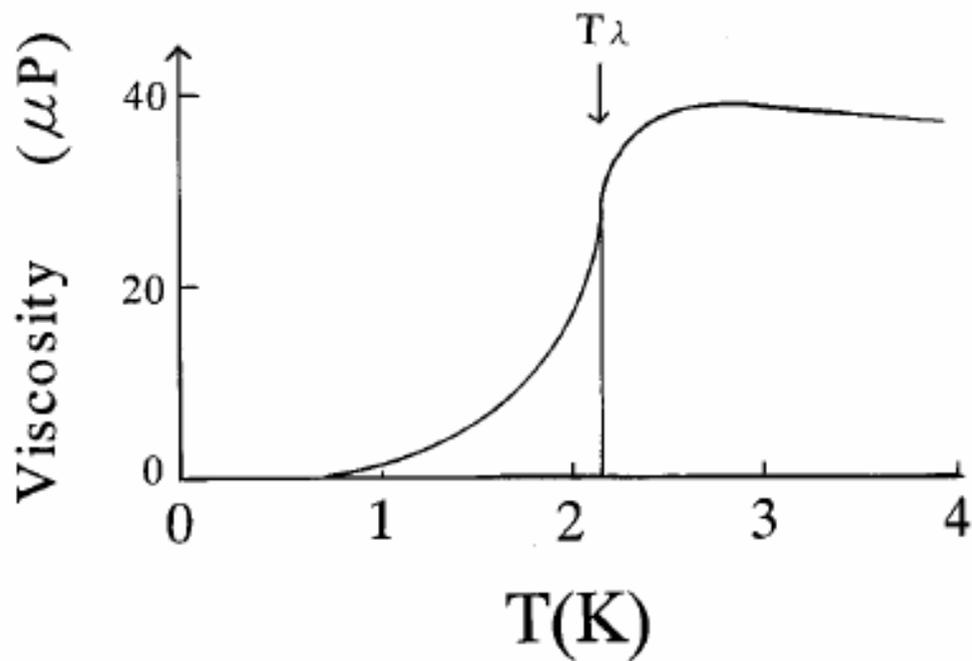
l'hélium superfluide
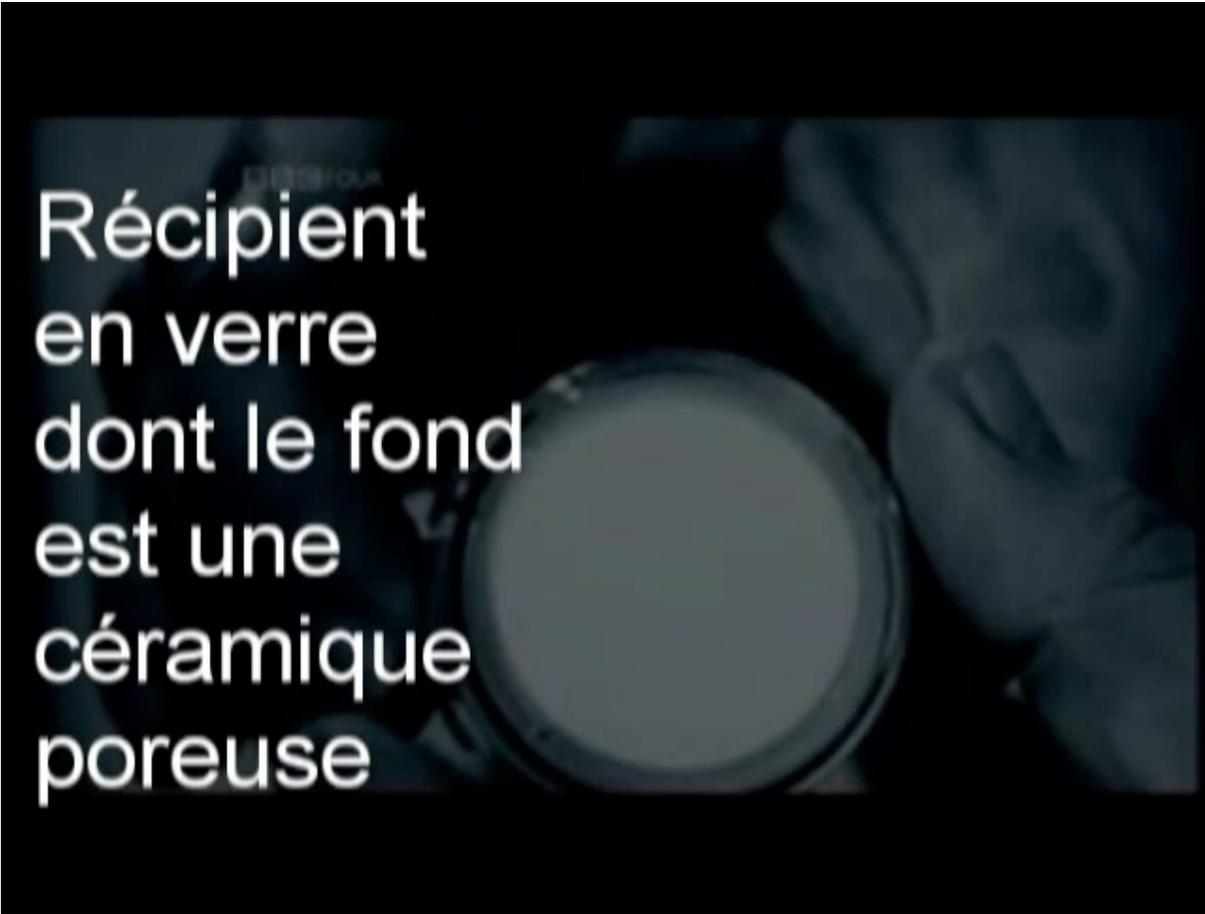
Récipient en verre dont le fond est une céramique poreuse

l'hélium superfluide

Une soucoupe remplie d'hélium superfluide

l'hélium superfluide
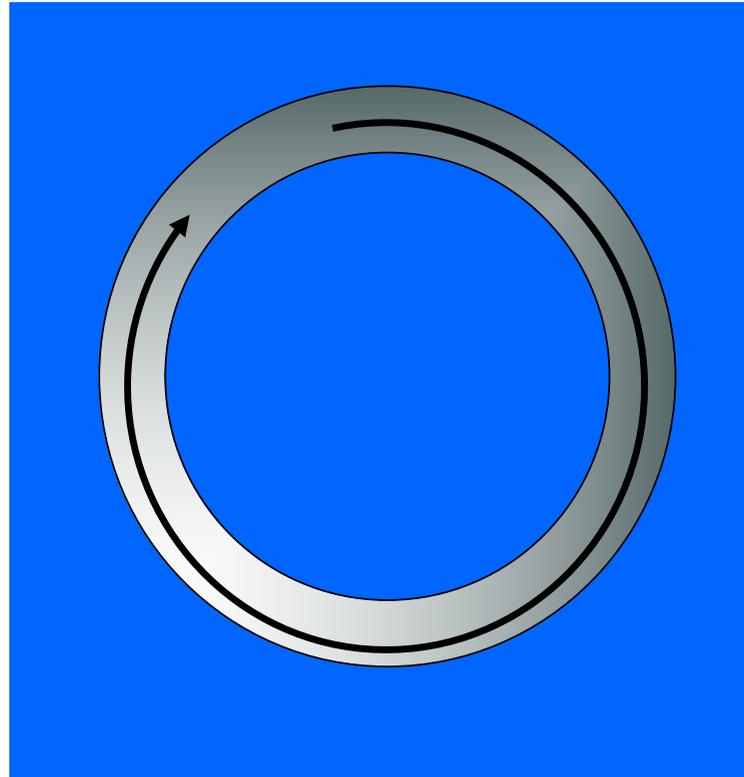
mouvement perpétuel

l'hélium superfluide

superfluidité : l'explication

les atomes forment soudain un condensat quantique.
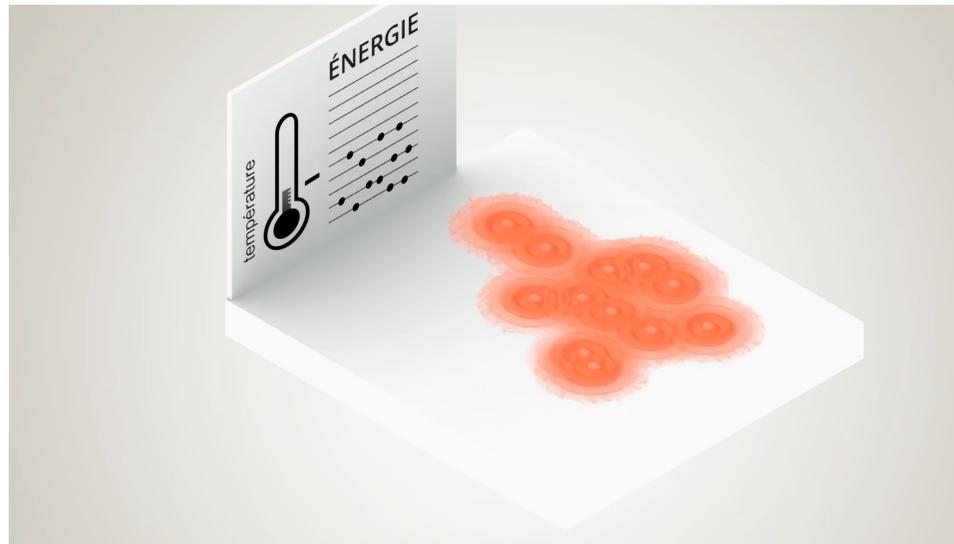
utiliser l'hélium pour aller sous 1K

Les cryostats à dilution

utiliser l'hélium pour aller sous 1K
Les cryostats à dilution
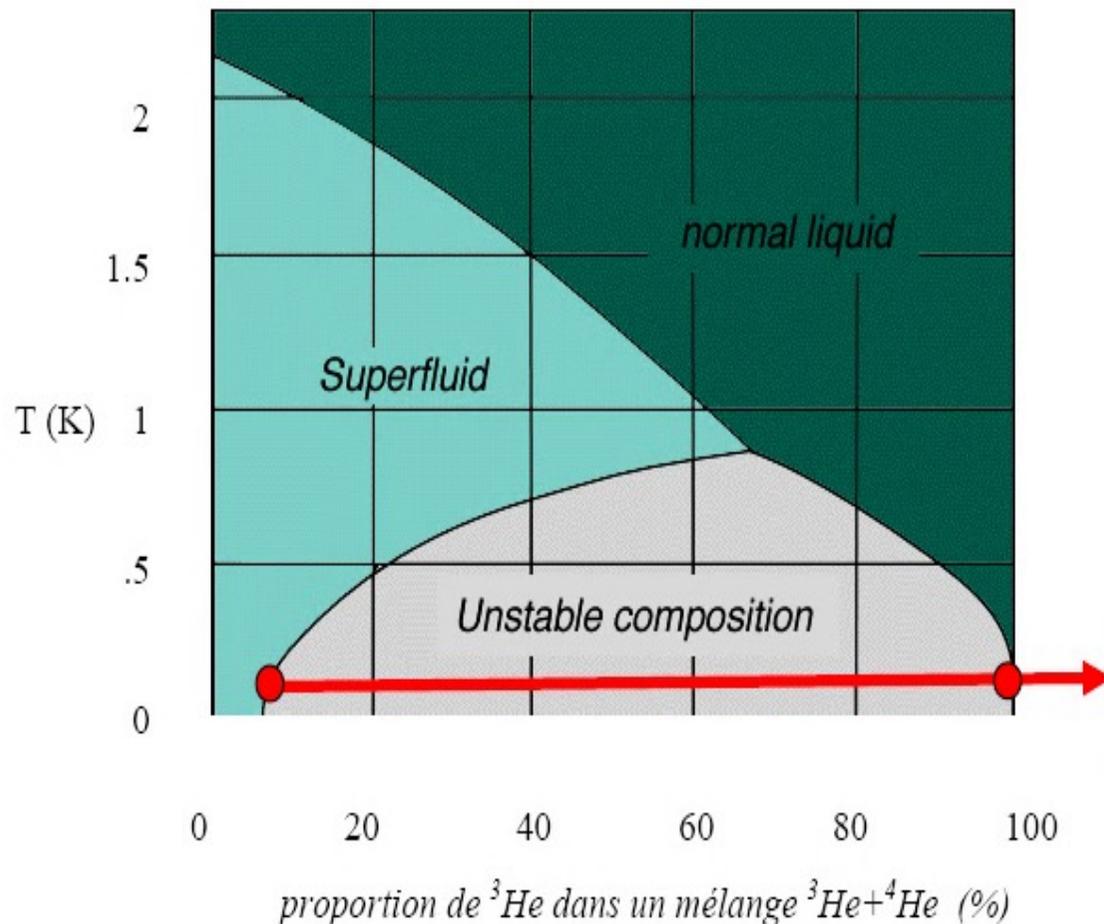
À très basse température,
2 phases coexistent,
l'une 100% ^{3}He et l'autre mélangée

utiliser l'hélium pour aller sous 1K
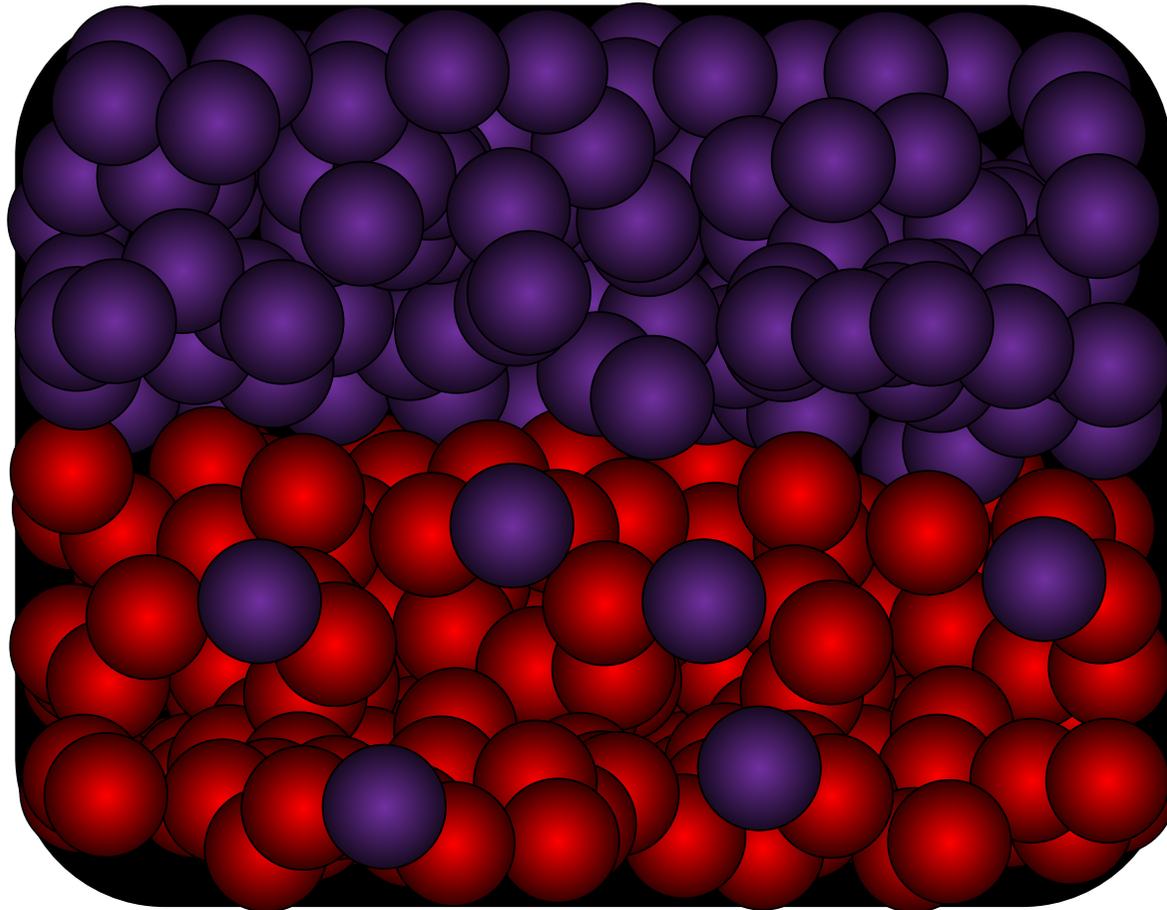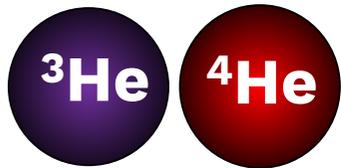
Les cryostats à dilution

³He   ⁴He

pompage
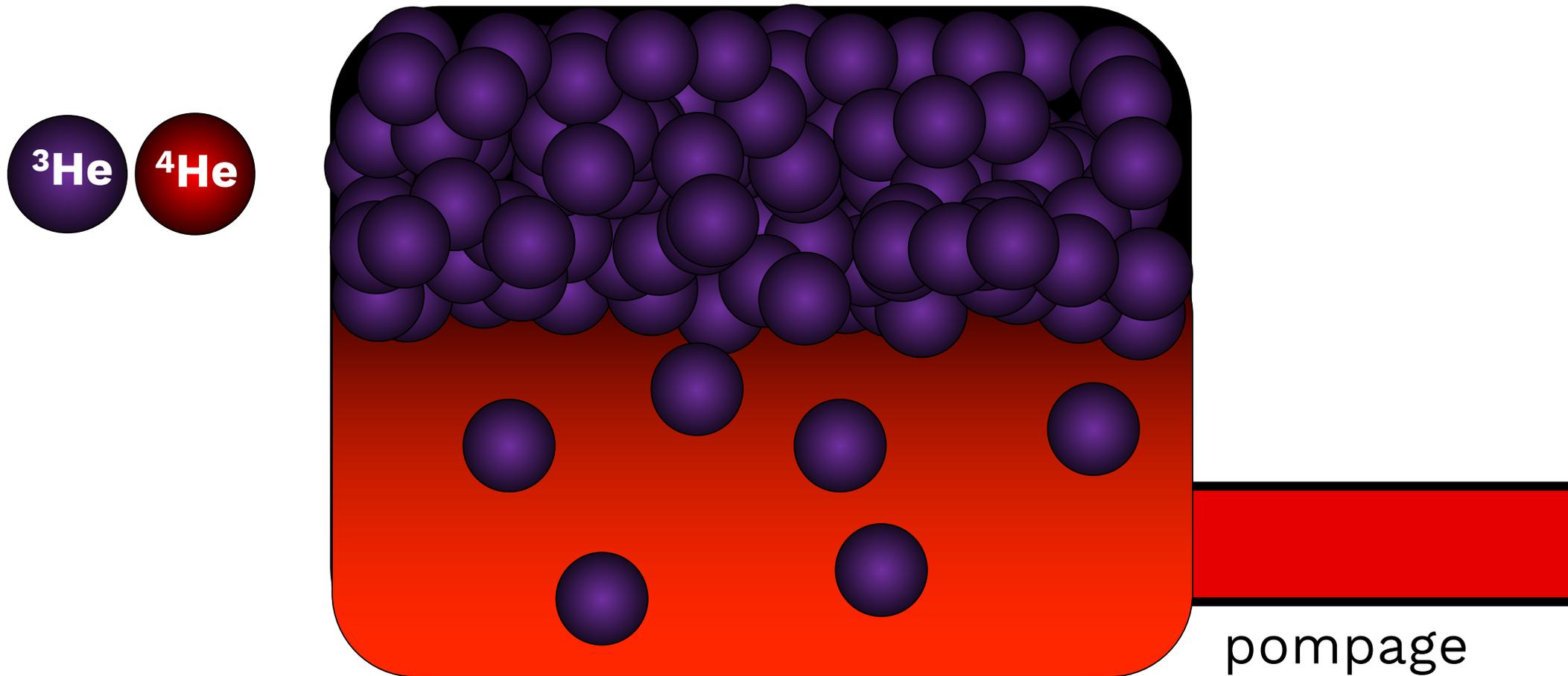
utiliser l'hélium pour aller sous 1K
Les cryostats à dilution
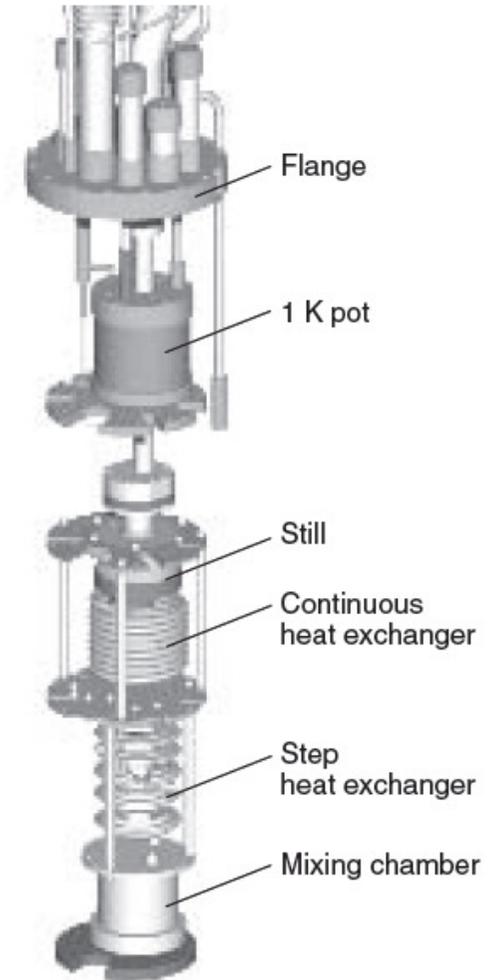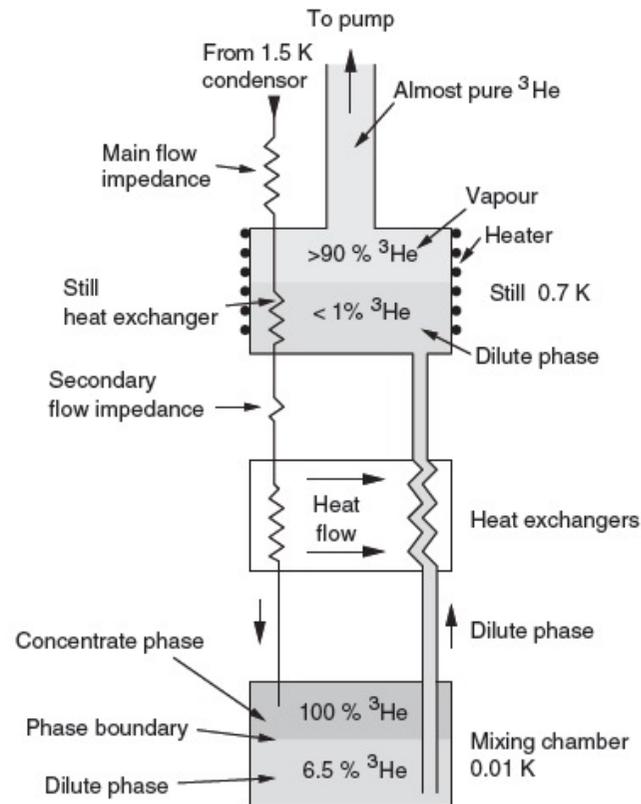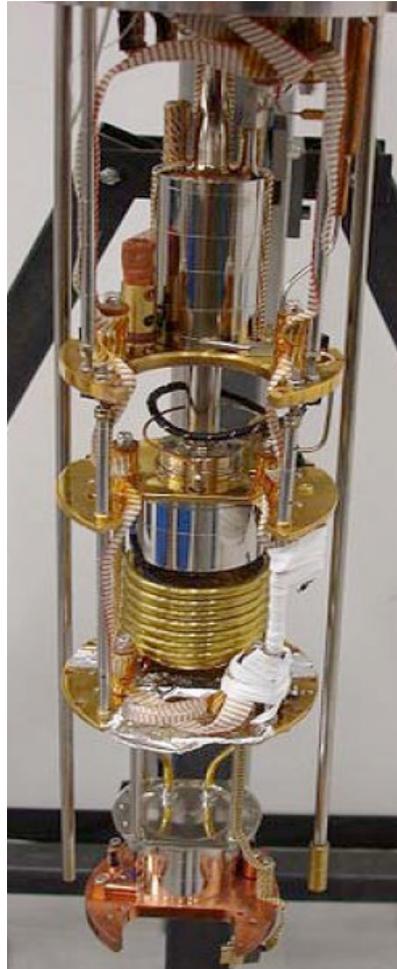
utiliser l'hélium pour aller sous 1K
Les cryostats à dilution

Record : T=1,7 mK (Univ. Lancaster)
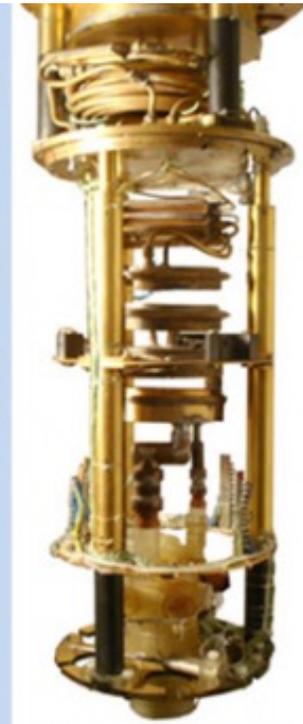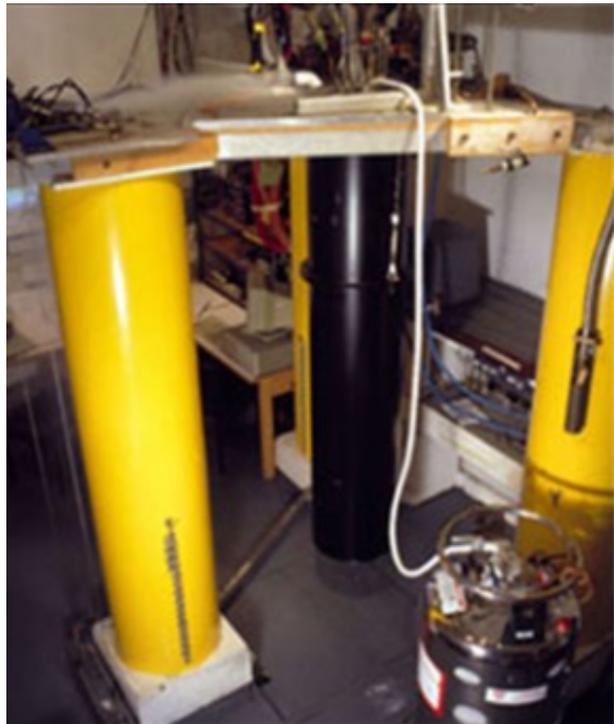
La température

recherches récentes

recherches récentes

1. le record du froid

2. refroidir et voir la quantique

3. mesurer la température à petite échelle

4. refroidir pour mesurer dans l'espace

5. le froid pour observer le vivant

recherches récentes

1. **le record du froid**

2. refroidir et voir la quantique

3. mesurer la température à petite échelle

4. refroidir pour mesurer dans l'espace

5. le froid pour observer le vivant

Polarized Nuclei in Normal and Superconducting Rhodium

T. A. Knuuttila,[1,]* J. T. Tuoriniemi,[1] K. Lefmann,[2] K. I. Juntunen,[1]
F. B. Rasmussen,[3] and K. K. Nummila[1,]†

[1]*Low Temperature Laboratory, Helsinki University of Technology,*
P.O. Box 2200, FIN-02015 HUT, Finland
[2]*Dept. Cond. Matt. Phys. and Chem., Risø National Laboratory, 4000 Roskilde, Denmark*
[3]*Niels Bohr Institute, University of Copenhagen,*
Universitetsparken 5, 2100 København Ø, Denmark

(Received September 27, 2000; revised December 27, 2000)

We performed SQUID-NMR measurements on a rhodium single crystal at ultra-low nuclear-spin temperatures. With initial polarizations up to $p = 0.95$, the antiferromagnetic tendency was clear, but surprisingly no indication of actual nuclear magnetic ordering was obtained. The lowest nuclear temperatures achieved were below 100 pK, whereas the lowest directly measured temperature was 280 pK. Double-spin-flip and evidence for triple-spin-flip resonance lines were detected, yielding direct information of the interactions between the nuclear spins. The superconducting transition of rhodium was observed with the critical values, $T_c = 210 \mu K$ and $B_c(0) = 3.4 \mu T$. For the first time, measurements with substantially correlated nuclei were performed in the superconducting state, where the effect of the coherent electron system on the spin-lattice relaxation rate was studied. The spin-lattice relaxation time was longer in the superconducting state at all temperatures and displayed a strong dependence on nuclear susceptibility.

1. INTRODUCTION

1.1. Background

Studies of nuclear magnetic ordering in metals have become experimentally feasible by the development of advanced cooling techniques, and thereby the spontaneously ordered phase of the nuclear spins has been observed in a few metals in the nano- and microkelvin regime.[1] The starting point for the theoretical understanding of nuclear magnets is usually

*E-mail: tauno.knuuttila@hut.fi
†Present address: VTT Automation, Measurement Technology, P.O. Box 1304, FIN-02044 VTT, Finland.

Knuuttila et al. *J. Low Temp. Phys.* (2001)

Helsinki, Finlande

2001

Refroidissement des noyaux du Rhodium à T=0,25 nK

utiliser l'hélium pour aller sous 1 mK

La desaimantation adiabatique
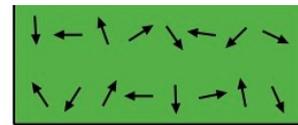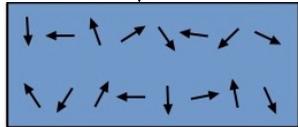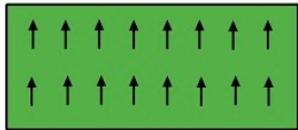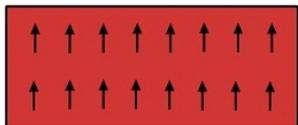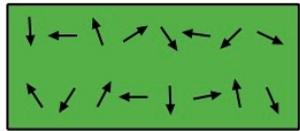
1. On applique un champ au métal.
   Ça oriente les spins de ses noyaux

2. On évacue la chaleur puis on isole

3. On éteint le champ : les spins se desordonnent, mais pas d'échange de chaleur avec l'extérieur. Pour permettre le desordre, le métal doit pomper de la chaleur sur lui-même : il refroidit.

utiliser l'hélium pour aller sous 1 mK

La desaimantation adiabatique

On « refroidit » les spins des noyaux des atomes du Rhodium.
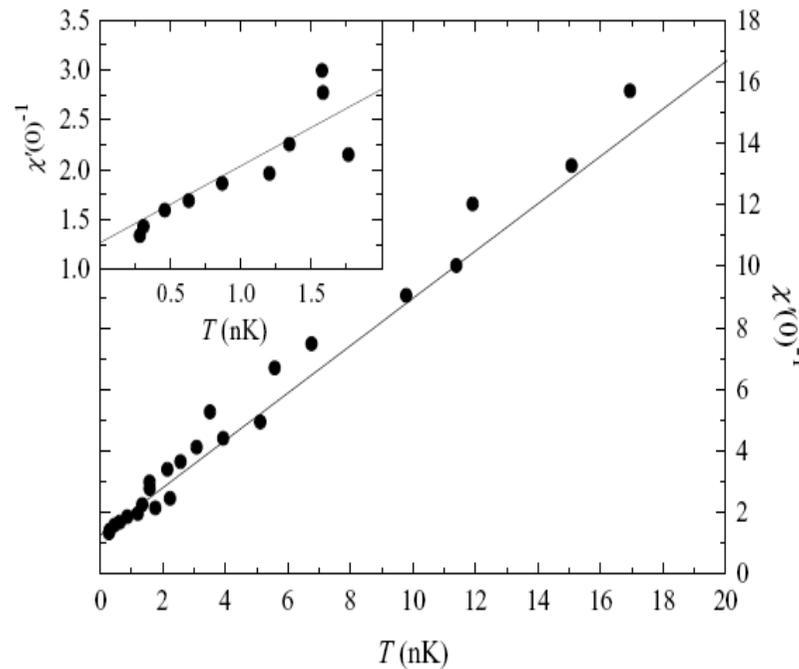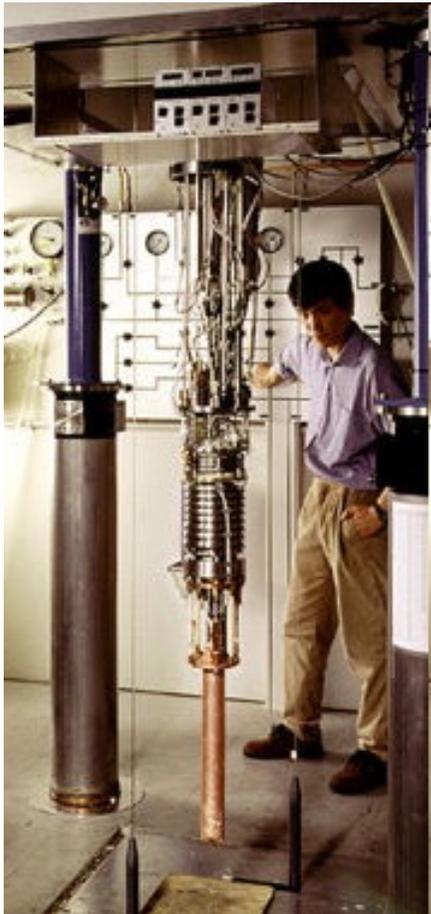
record : T = 200 pK

Attention, ces températures sont celles des spins des noyaux (les électrons, eux, restent en gros à 0.1mK)

recherches récentes

1. le record du froid

2. mesurer la température à petite échelle

3. refroidir et voir la quantique

4. refroidir pour mesurer dans l'espace

5. le froid pour observer le vivant

Nanometre-scale thermometry in a living cell

G. Kucsko[1]*, P. C. Maurer[1]*, N. Y. Yao[1], M. Kubo[2], H. J. Noh[3], P. K. Lo[4], H. Park[1,2,3] & M. D. Lukin[1]

Sensitive probing of temperature variations on nanometre scales is an outstanding challenge in many areas of modern science and technology[1]. In particular, a thermometer capable of subdegree temperature resolution over a large range of temperatures as well as integration within a living system could provide a powerful new tool in many areas of biological, physical and chemical research. Possibilities range from the temperature-induced control of gene expression[2–5] and tumour metabolism[6] to the cell-selective treatment of disease[7,8] and the study of heat dissipation in integrated circuits[1]. By combining local light-induced heat sources with sensitive nanoscale thermometry, it may also be possible to engineer biological processes at the subcellular level[2–5]. Here we demonstrate a new approach to nanoscale thermometry that uses coherent manipulation of the electronic spin associated with nitrogen–vacancy colour centres in diamond. Our technique makes it possible to detect temperature variations as small as 1.8 mK (a sensitivity of 9 mK Hz$^{-1/2}$) in an ultrapure bulk diamond sample. Using nitrogen–vacancy centres in diamond nanocrystals (nanodiamonds), we directly measure the local thermal environment on length scales as short as 200 nanometres. Finally, by introducing both nanodiamonds and gold nanoparticles into a single human embryonic fibroblast, we demonstrate temperature-gradient control and mapping at the subcellular level, enabling unique potential applications in life sciences.

Many promising approaches to local temperature sensing[1] are being explored at present. These include scanning probe microscopy[1,9], Raman spectroscopy[10], and fluorescence-based measurements using nanoparticles[11,12] and organic dyes[13,14]. Fluorescent polymers[13] and green fluorescent proteins[14] have recently been used for temperature mapping within a living cell. However, many of these existing methods are limited by drawbacks such as low sensitivity and systematic errors due to fluctuations in the fluorescence rate[11,12], the local chemical environment[13] and the optical properties of the surrounding medium[14]. Moreover, although promising, methods based on green fluorescent proteins rely on cellular transfection[14] that proves to be difficult to achieve in certain primary cell types[15]. Our new approach to nanoscale thermometry uses the quantum mechanical spin associated with nitrogen–vacancy colour centres in diamond. As illustrated in Fig. 1b, in its electronic ground state each nitrogen–vacancy centre constitutes a spin-1 system. These spin states can be coherently manipulated using microwave pulses and efficiently initialized and detected by means of laser illumination (Supplementary Information). In the absence of an external magnetic field, the precise value of the transition frequency
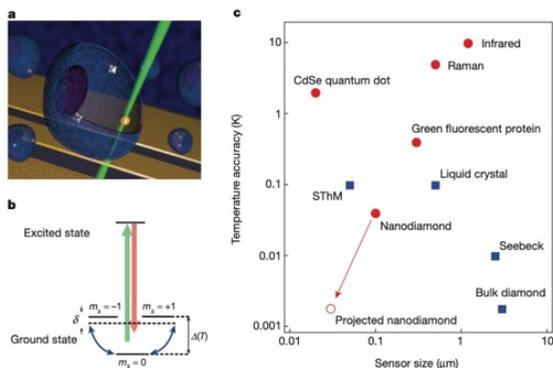
Figure 1 | Nitrogen–vacancy-based nanoscale thermometry. a, Schematic image depicting nanodiamonds (grey diamonds) and a gold nanoparticle (yellow sphere) within a living cell (central blue object; others are similar) with coplanar waveguide (yellow stripes) in the background. The controlled application of local heat is achieved by laser illumination of the gold nanoparticle, and nanoscale thermometry is achieved by precision spectroscopy of the nitrogen–vacancy spins in the nanodiamonds. **b**, Simplified nitrogen–vacancy level diagram showing a ground-state spin triplet and an excited state. At zero magnetic field, the $|\pm1\rangle$ sublevels are split from the $|0\rangle$ state by a temperature-dependent zero field splitting $\Delta(T)$. Pulsed microwave radiation is applied (detuning, δ) to perform Ramsey-type spectroscopy. **c**, Comparison of sensor sizes and temperature accuracies for the nitrogen–vacancy quantum thermometer and other reported techniques. Red circles indicate methods that are biologically compatible. The open red circle indicates the ultimate expected accuracy for our measurement technique in solution (Methods).

[1]Department of Physics, Harvard University, Cambridge, Massachusetts 02138, USA. [2]Department of Chemistry and Chemical Biology, Harvard University, Cambridge, Massachusetts 02138, USA. [3]Broad Institute of MIT and Harvard University, 7 Cambridge Center, Cambridge, Massachusetts 02142, USA. [4]Department of Biology and Chemistry, City University of Hong Kong, Tat Chee Avenue, Kowloon, Hong Kong SAR, China.
*These authors contributed equally to this work.

Kucsko, Georg, et al. *Nature* (2013)	
Harvard, USA	
2021	
conception d'un thermomètre nanométrique dans une cellule vivante.	

mesurer la température à petite échelle

mesurer la température à petite échelle
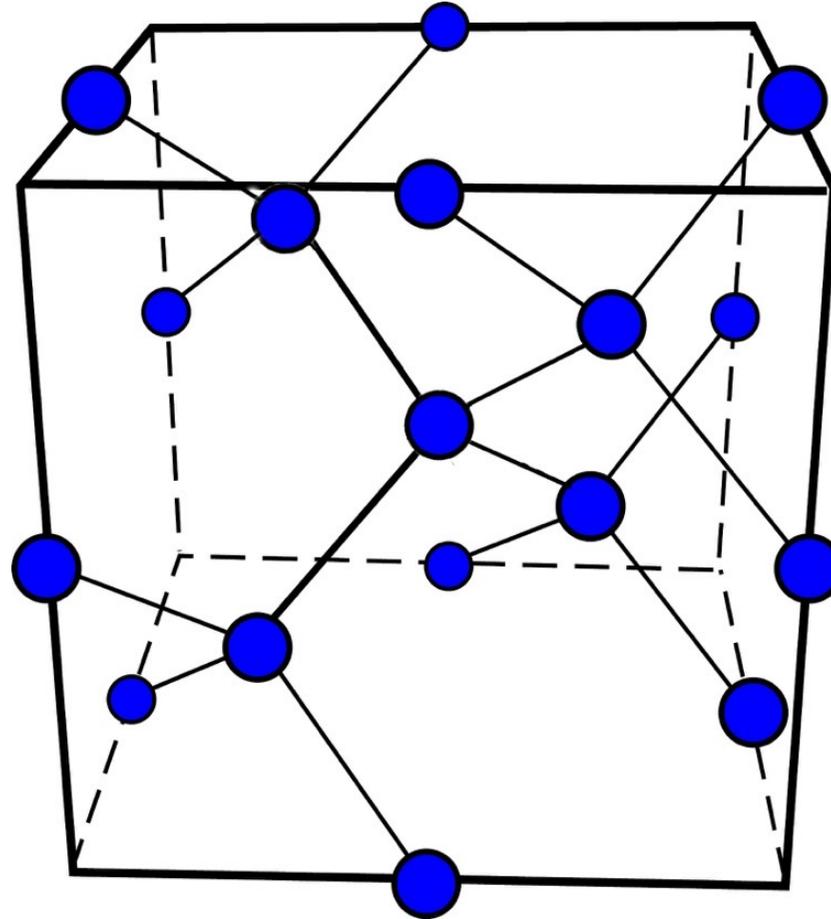
mesurer la température à petite échelle
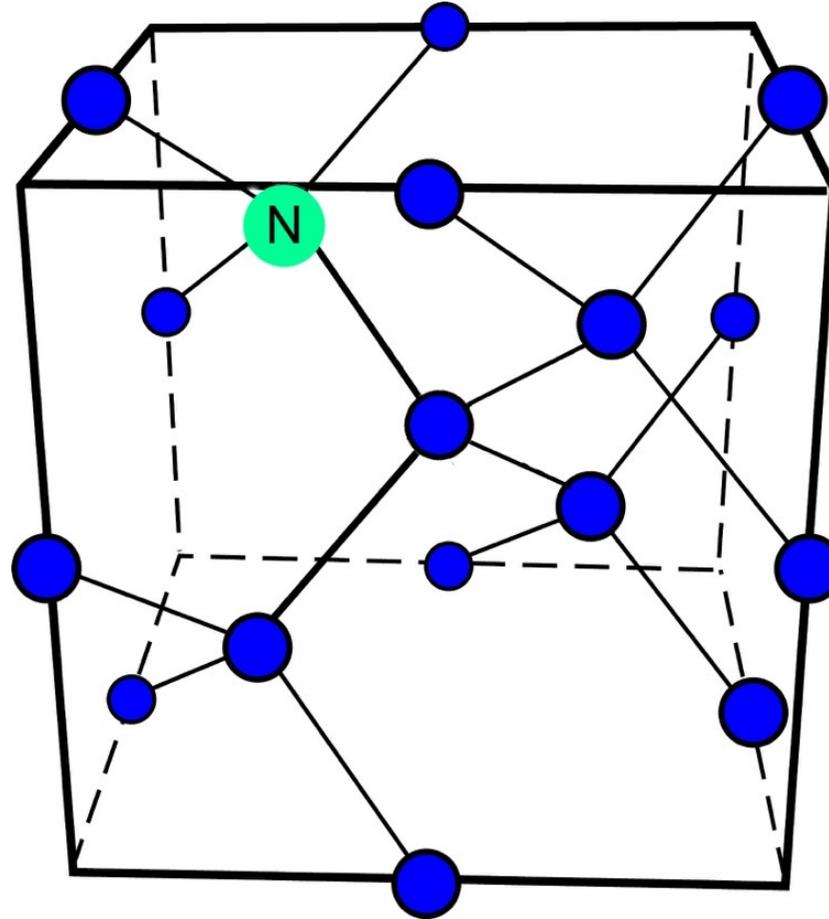
mesurer la température à petite échelle
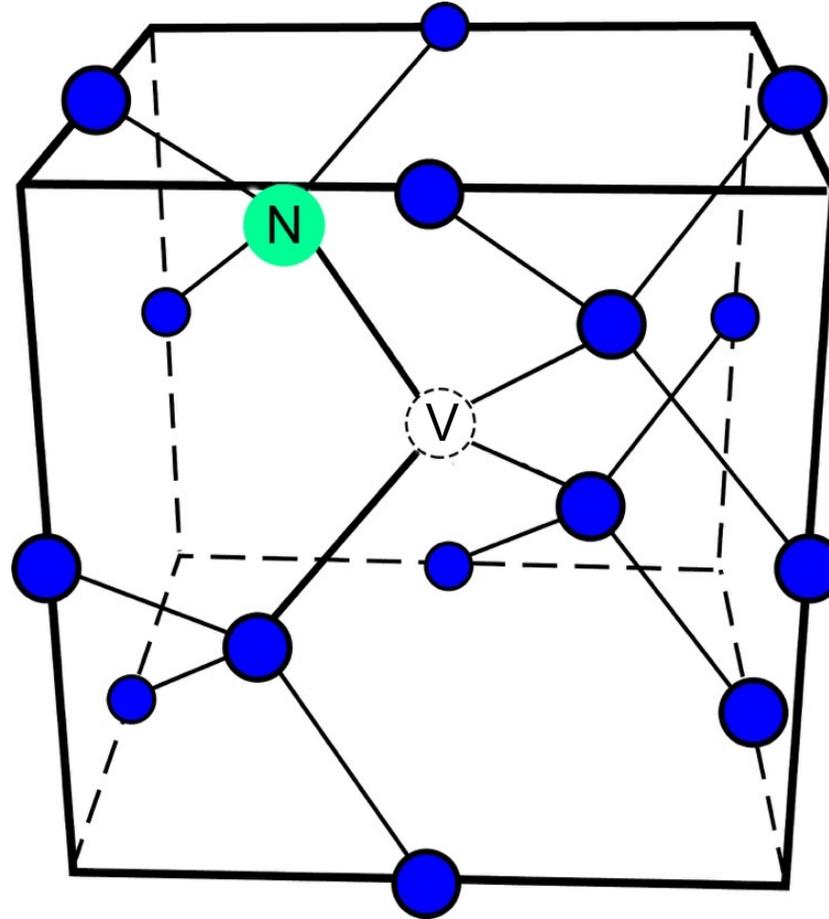
« Un centre NV »
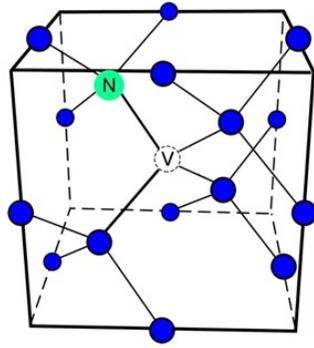
mesurer la température à petite échelle

On mesure la fréquence à laquelle le spin du centre NV résonne par le changement de fluorescence

La position de la résonance dépend de la température
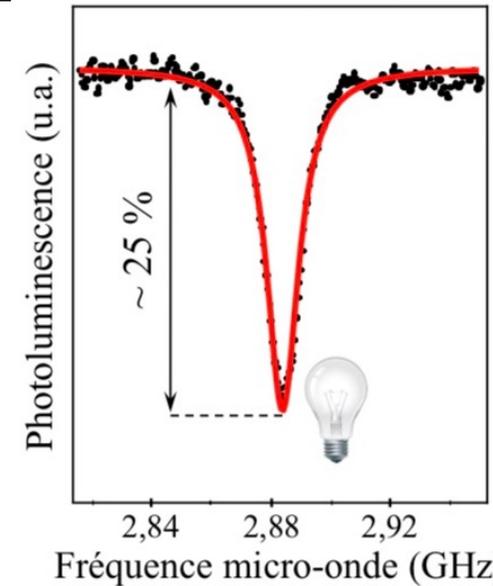
@Toraille
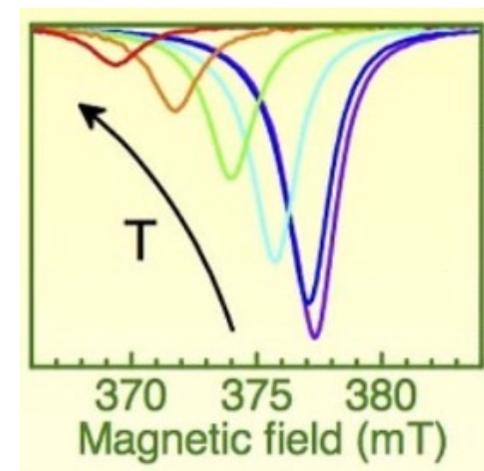
mesurer la température à petite échelle

- on peut mesurer localement la température.
- On distingue des différences de température de 0,1K sur quelques µm
- exemple d'application : traitements contre le cancer
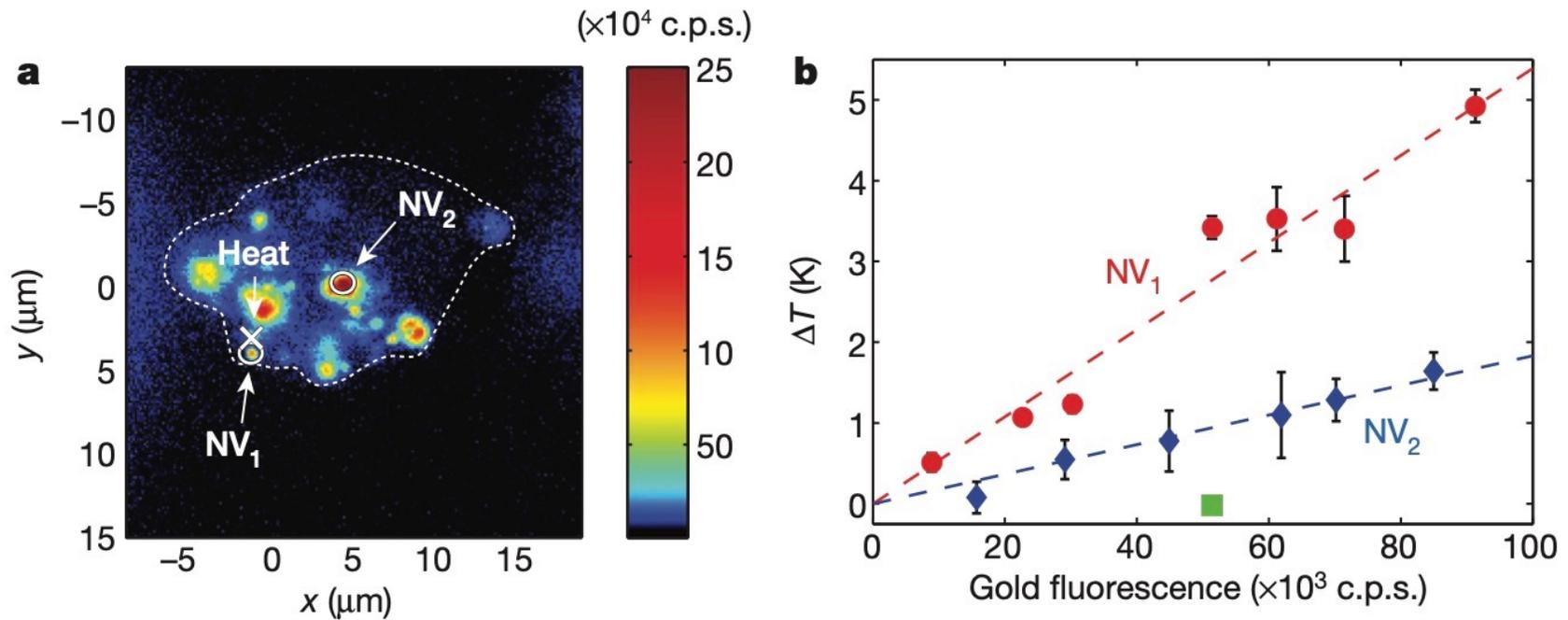
recherches récentes

1. le record du froid

2. mesurer la température à petite échelle

3. refroidir et voir la quantique

4. refroidir pour mesurer dans l'espace

5. le froid pour observer le vivant

ARTICLE

Check for updates

A macroscopic object passively cooled into its quantum ground state of motion beyond single-mode cooling

D. Cattiaux[1], I. Golokolenov [1], S. Kumar[1], M. Sillanpää[2], L. Mercier de Lépinay[2], R. R. Gazizulin [1], X. Zhou [3], A. D. Armour[4], O. Bourgeois[1], A. Fefferman[1] & E. Collin [1]✉

The nature of the quantum-to-classical crossover remains one of the most challenging open question of Science to date. In this respect, moving objects play a specific role. Pioneering experiments over the last few years have begun exploring quantum behaviour of micron-sized mechanical systems, either by passively cooling single GHz modes, or by adapting laser cooling techniques developed in atomic physics to cool specific low-frequency modes far below the temperature of their surroundings. Here instead we describe a very different approach, passive cooling of a whole micromechanical system down to 500 μK, reducing the average number of quanta in the fundamental vibrational mode at 15 MHz to just 0.3 (with even lower values expected for higher harmonics); the challenge being to be still able to detect the motion without disturbing the system noticeably. With such an approach higher harmonics and the surrounding environment are also cooled, leading to potentially much longer mechanical coherence times, and enabling experiments questioning mechanical wave-function collapse, potentially from the gravitational background, and quantum thermo-dynamics. Beyond the average behaviour, here we also report on the fluctuations of the fundamental vibrational mode of the device in-equilibrium with the cryostat. These reveal a surprisingly complex interplay with the local environment and allow characteristics of two distinct thermodynamic baths to be probed.

[1] Univ. Grenoble Alpes, Institut Néel - CNRS UPR2940, 25 rue des Martyrs, BP 166, 38042 Grenoble Cedex 9, France. [2] Departement of Applied Physics, Aalto University, FI-00076 Aalto, Finland. [3] IEMN, Univ. Lille - CNRS UMR8520, Av. Henri Poincaré, Villeneuve d'Ascq 59650, France. [4] Centre for the Mathematics and Theoretical Physics of Quantum Non-Equilibrium Systems and School of Physics and Astronomy, University of Nottingham, Nottingham NG7 2RD, United Kingdom. ✉email: eddy.collin@neel.cnrs.fr

Cattiaux et al., Nature Com., 2021

Grenoble

2021

mesure du mouvement quantique d'un objet jusqu'à 0,5mK

- on refroidit un objet à 0,5 mK
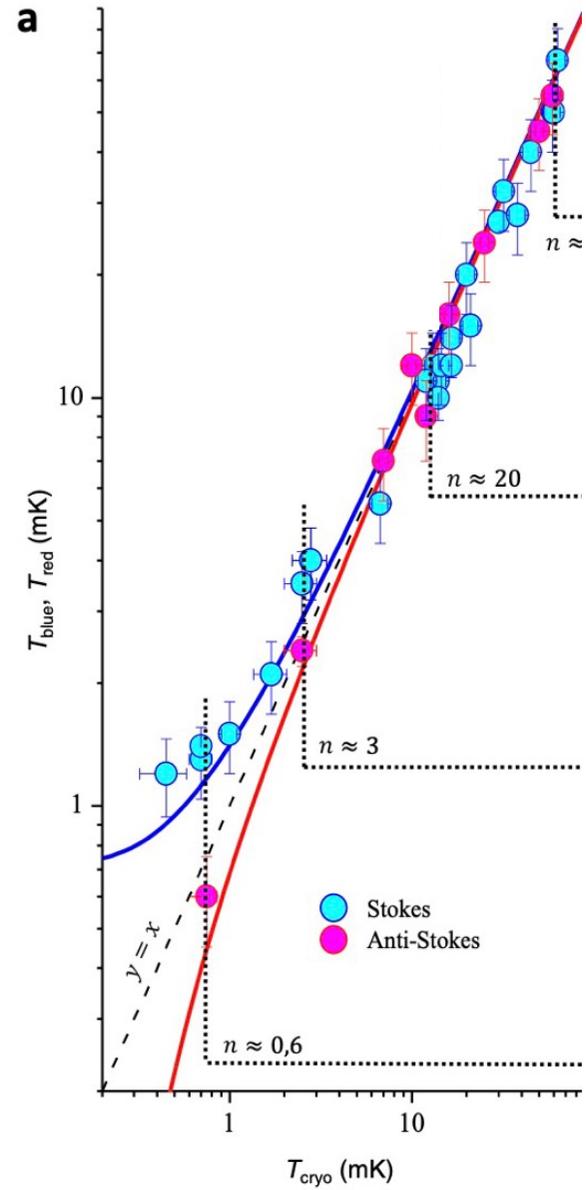
on mesure comment il bouge en comptant le nombre de phonons (vibrations collectives des atomes
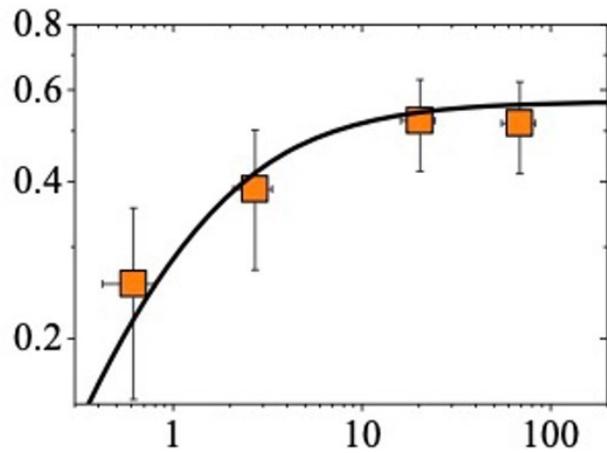
nombre de phonons
(vibrations des atomes)
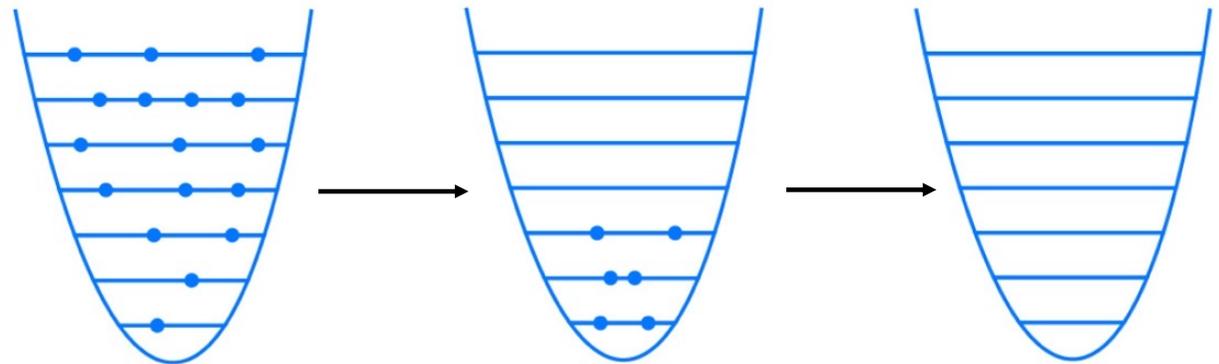
la température décroit :
les phonons disparaissent

à 0,5mK, plus aucun mouvement collectif : le système a atteint son « état quantique fondamental »

recherches récentes

1. le record du froid

2. mesurer la température à petite échelle

3. refroidir et voir la quantique

4. refroidir pour mesurer dans l'espace

5. le froid pour observer le vivant

Astronomy
&
Astrophysics

Special feature

Planck 2013 results. I. Overview of products and scientific results

Planck Collaboration: P. A. R. Ade[116], N. Aghanim[79], M. I. R. Alves[79], C. Armitage-Caplan[122], M. Arnaud[96], M. Ashdown[93,8], F. Atrio-Barandela[23], J. Aumont[79], H. Aussel[96], C. Baccigalupi[114], A. J. Banday[128,13], R. B. Barreiro[89], R. Barrena[88], M. Bartelmann[126,103], J. G. Bartlett[1,91], N. Bartolo[43], S. Basak[114], E. Battaner[131], R. Battye[92], K. Benabed[80,125], A. Benoît[77], A. Benoit-Lévy[32,80,125], J.-P. Bernard[128,13], M. Bersanelli[47,68], B. Bertincourt[79], M. Bethermin[96], P. Bielewicz[128,13,114], I. Bikmaev[27,3], A. Blanchard[128], J. Bobin[96], J. J. Bock[91,14], H. Böhringer[104], A. Bonaldi[92], L. Bonavera[89], J. R. Bond[11], J. Borrill[18,119], F. R. Bouchet[80,125], F. Boulanger[79], H. Bourdin[49], J. W. Bowyer[75], M. Bridges[93,8,85], M. L. Brown[92], M. Bucher[1], R. Burenin[118,107], C. Burigana[67,45], R. C. Butler[67], E. Calabrese[122], B. Cappellini[68], J.-F. Cardoso[97,1,80], R. Carr[54], P. Carvalho[8], M. Casale[54], G. Castex[1], A. Catalano[98,95], A. Challinor[85,93,15], A. Chamballu[96,20,79], R.-R. Chary[76], X. Chen[76], H. C. Chiang[37,9], L.-Y Chiang[84], G. Chon[104], P. R. Christensen[110,51], E. Churazov[103,118], S. Church[121], M. Clemens[63], D. L. Clements[75], S. Colombi[80,125], L. P. L. Colombo[31,91], C. Combet[98], B. Comis[98], F. Couchot[94], A. Coulais[95], B. P. Crill[91,111], M. Cruz[25], A. Curto[8,89], F. Cuttaia[67], A. Da Silva[16], H. Dahle[87], L. Danese[114], R. D. Davies[92], R. J. Davis[92], P. de Bernardis[46], A. de Rosa[67], G. de Zotti[63,114], T. Déchelette[80], J. Delabrouille[1], J.-M. Delouis[80,125], J. Démoclès[96], F.-X. Désert[72], J. Dick[114], C. Dickinson[92], J. M. Diego[89], K. Dolag[130,103], H. Dole[79,78], S. Donzelli[68], O. Doré[91,14], M. Douspis[79], A. Ducout[80], J. Dunkley[122], X. Dupac[55], G. Efstathiou[85], F. Elsner[80,125], T. A. Enßlin[103], H. K. Eriksen[87], O. Fabre[80], E. Falgarone[95], M. C. Falvella[6], Y. Fantaye[87], J. Fergusson[15], C. Filliard[94], F. Finelli[67,69], I. Flores-Cacho[13,128], S. Foley[56], O. Forni[128,13], P. Fosalba[81], M. Frailis[65], A. A. Fraisse[37], E. Franceschi[67], M. Freschi[55], S. Fromenteau[1,79], M. Frommert[22], T. C. Gaier[91], S. Galeotta[65], J. Gallegos[55], S. Galli[80], K. Ganga[1], C. Gauthier[1,101], R. T. Génova-Santos[88], T. Ghosh[79], M. Giard[128,13], G. Giardino[56], M. Gilfanov[103,118], D. Girard[98], Y. Giraud-Héraud[1], E. Gjerløw[87], J. González-Nuevo[89,114], K. M. Górski[91,132], S. Gratton[93,85], A. Gregorio[48,65], A. Gruppuso[67], J. E. Gudmundsson[37], J. Haissinski[94], J. Hamann[124], F. K. Hansen[87], M. Hansen[110], D. Hanson[105,91,11], D. L. Harrison[85,93], A. Heavens[75], G. Helou[14], A. Hempel[88,52], S. Henrot-Versillé[94], C. Hernández-Monteagudo[17,103], D. Herranz[89], S. R. Hildebrandt[14], E. Hivon[80,125], S. Ho[34], M. Hobson[8], W. A. Holmes[91], A. Hornstrup[21], Z. Hou[40], W. Hovest[103], G. Huey[42], K. M. Huffenberger[35], G. Hurier[79,98], A. H. Jaffe[75], T. R. Jaffe[128,13], J. Jasche[80], J. Jewell[91], W. C. Jones[37], M. Juvela[36], P. Kalberla[7], P. Kangaslahti[91], E. Keihänen[36], J. Kerp[7], R. Keskitalo[29,18], I. Khamitov[123,27], K. Kiiveri[36,61], J. Kim[110], T. S. Kisner[100], R. Kneissl[53,10], J. Knoche[103], L. Knox[40], M. Kunz[22,79,4], H. Kurki-Suonio[36,61], F. Lacasa[79], G. Lagache[79], A. Lähteenmäki[2,61], J.-M. Lamarre[95], M. Langer[79], A. Lasenby[8,93], M. Lattanzi[45], R. J. Laureijs[57], A. Lavabre[94], C. R. Lawrence[91], M. Le Jeune[1], S. Leach[114], J. P. Leahy[92], R. Leonardi[55], J. León-Tavares[58,2], C. Leroy[79,128,13], J. Lesgourgues[124,113], A. Lewis[33], A. Li[102,103], A. Liddle[115,33], M. Liguori[43], P. B. Lilje[87], M. Linden-Vørnle[21], V. Lindholm[36,61], M. López-Caniego[89], S. Lowe[92], P. M. Lubin[41], J. F. Macías-Pérez[98], C. J. MacTavish[93], B. Maffei[92], G. Maggio[65], D. Maino[47,68], N. Mandolesi[67,6,45], A. Mangilli[80], A. Marcos-Caballero[89], D. Marinucci[50], M. Maris[65], F. Marleau[83], D. J. Marshall[96], P. G. Martin[11], E. Martínez-González[89], S. Masi[46], M. Massardi[66], S. Matarrese[43], T. Matsumura[14], F. Matthai[103], L. Maurin[1], P. Mazzotta[49], A. McDonald[56], J. D. McEwen[32,108], P. McGehee[76], S. Mei[59,127,14], P. R. Meinhold[41], A. Melchiorri[46,70], J.-B. Melin[20], L. Mendes[55], E. Menegoni[46], A. Mennella[47,68], M. Migliaccio[85,93], K. Mikkelsen[87], M. Millea[40], S. Mitra[74,91], M.-A. Miville-Deschênes[79,11], D. Molinari[44,67], A. Moneti[80], L. Montier[128,13], G. Morgante[67], N. Morisset[56], D. Mortlock[75], A. Moss[117], D. Munshi[116], J. A. Murphy[109], P. Naselsky[110,51], F. Nati[46], P. Natoli[45,5,67], M. Negrello[63], N. P. H. Nesvadba[79], C. B. Netterfield[26], H. U. Nørgaard-Nielsen[21], C. North[116], F. Noviello[92], D. Novikov[75], I. Novikov[110], I. J. O'Dwyer[91], S. Osborne[121], C. O'Sullivan[109], C. A. Oxborrow[21], F. Paci[114], L. Pagano[46,70], F. Pajot[79], R. Paladini[76], S. Pandolfi[49], D. Paoletti[67,69], B. Partridge[60], F. Pasian[65], G. Patanchon[1], P. Paykari[96], D. Pearson[91], T. J. Pearson[14,76], M. Peel[92], H. V. Peiris[32], O. Perdereau[94], L. Perotto[98], F. Perrotta[114], V. Pettorino[37], F. Piacentini[46], M. Piat[1], E. Pierpaoli[31], D. Pietrobon[91], S. Plaszczynski[94], P. Platania[90], D. Pogosyan[38], E. Pointecouteau[128,13], G. Polenta[5,64], N. Ponthieu[79,72], L. Popa[82], T. Poutanen[61,36,2], G. W. Pratt[96], G. Prézeau[14,91], S. Prunet[80,125], J.-L. Puget[79], A. R. Pullen[91], J. P. Rachen[28,103], B. Racine[1], A. Rahlin[37], C. Räth[104], W. T. Reach[129], R. Rebolo[88,19,52], M. Reinecke[103], M. Remazeilles[92,79,1], C. Renault[98], A. Renzi[114], A. Riazuelo[80,125], S. Ricciardi[67], T. Riller[103], C. Ringeval[86,80,125], I. Ristorcelli[128,13], G. Robbers[103], G. Rocha[91,14], M. Roman[1], C. Rosset[1], M. Rossetti[47,68], G. Roudier[1,95,91], M. Rowan-Robinson[75], J. A. Rubiño-Martín[88,52], B. Ruiz-Granados[131], B. Rusholme[76], E. Salerno[12], M. Sandri[67], L. Sanselme[98], D. Santos[98], M. Savelainen[36,61], G. Savini[112], B. M. Schaefer[126], F. Schiavon[67], D. Scott[30], M. D. Seiffert[91,14], P. Serra[79], E. P. S. Shellard[15], K. Smith[37], G. F. Smoot[39,100,1], T. Souradeep[74], L. D. Spencer[116], J.-L. Starck[96], V. Stolyarov[8,93,120], R. Stompor[1], R. Sudiwala[116], R. Sunyaev[103,118], F. Sureau[96], P. Sutter[80], D. Sutton[85,93], A.-S. Suur-Uski[36,61], J.-F. Sygnet[80], J. A. Tauber[57,*], D. Tavagnacco[65,48], D. Taylor[54], L. Terenzi[67], D. Texier[54], L. Toffolatti[24,89], M. Tomasi[68], J.-P. Torre[79], M. Tristram[94], J. Tucci[22,94], J. Tuovinen[106], M. Türler[73], M. Tuttlebee[56], G. Umana[62], L. Valenziano[67], J. Valiviita[61,36,87], B. Van Tent[99], J. Varis[106], L. Vibert[79], M. Viel[65,71], P. Vielva[89], F. Villa[67], N. Vittorio[49], L. A. Wade[91], B. D. Wandelt[80,125,42], C. Watson[56], R. Watson[92], I. K. Wehus[91], N. Welikala[1], J. Weller[130], M. White[39], S. D. M. White[103], A. Wilkinson[92], B. Winkel[7], J.-Q. Xia[114], D. Yvon[20], A. Zacchei[65], J. P. Zibin[30], and A. Zonca[41]

(Affiliations can be found after the references)

Received 21 March 2013 / Accepted 17 May 2014

* Corresponding author: e-mail: jtauber@cosmos.esa.int

Le fond diffus cosmologique
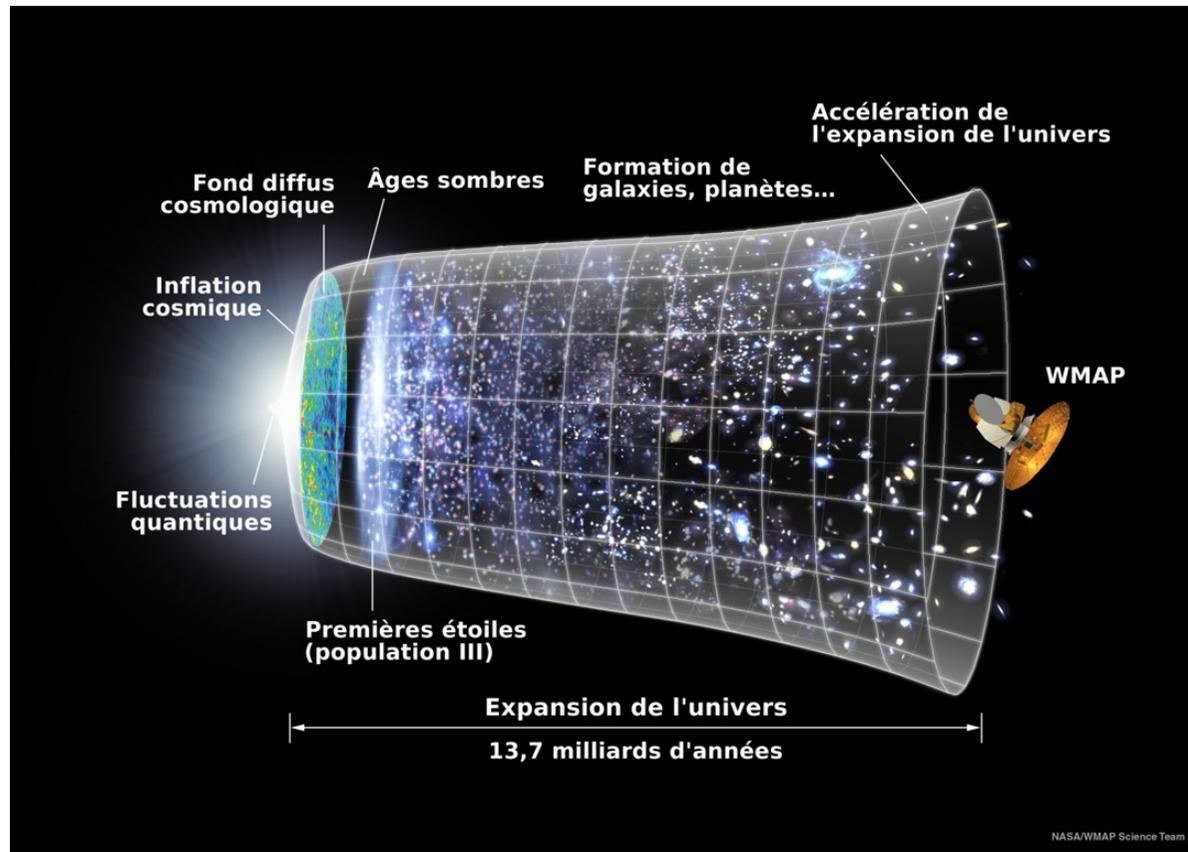
Rayonnement fossile datant du moment où l'Univers s'est suffisamment refroidi pour que la matière sorte de l'état de plasma et que les photons puissent nous atteindre (ce qui revient à dire que l'Univers devienne transparent) : a eu lieu 380 000 ans après le big bang

Le fond diffus cosmologique
mesure par le satelllite Planck
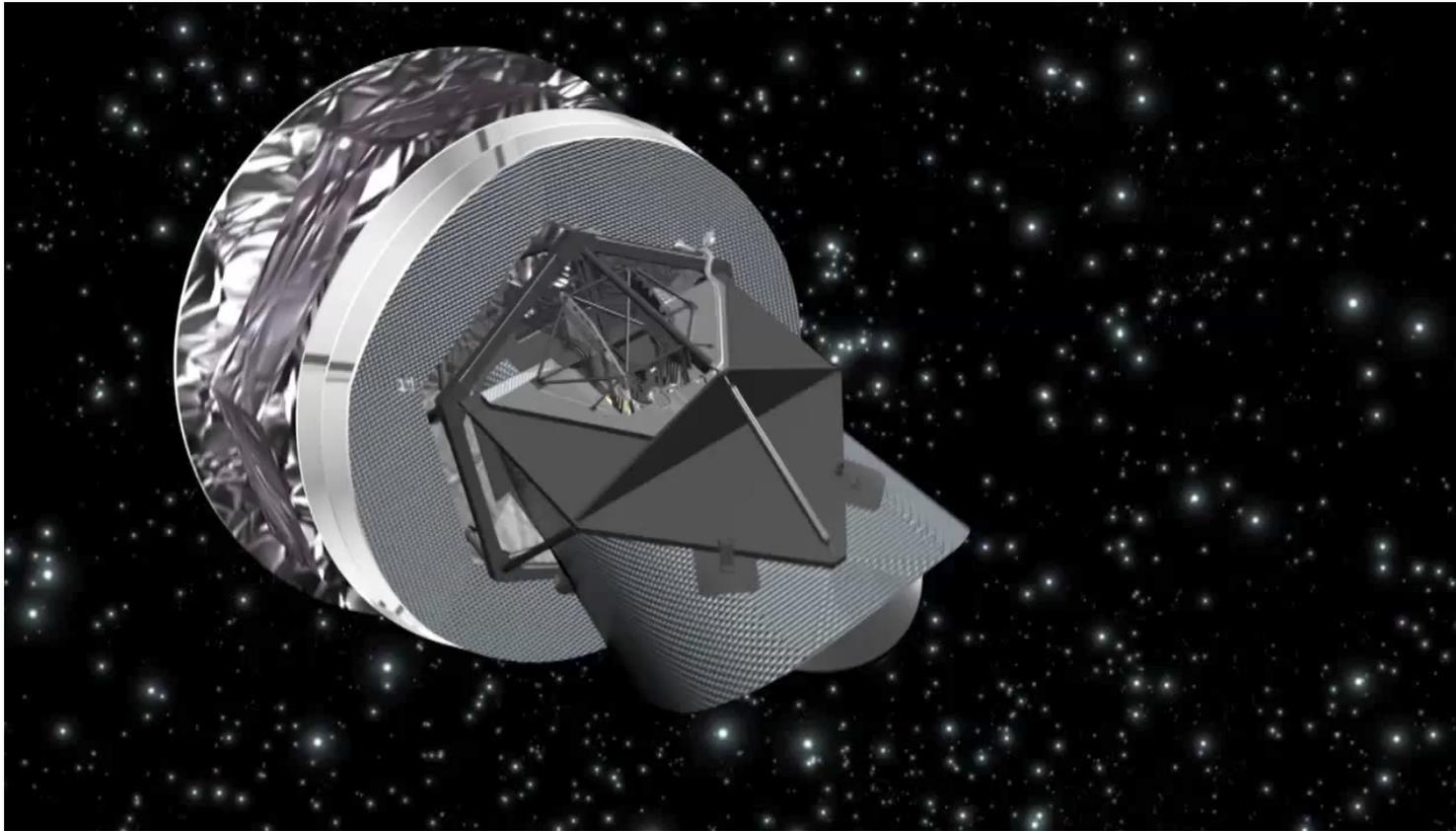
Le fond diffus cosmologique
mesure par le satelllite Planck
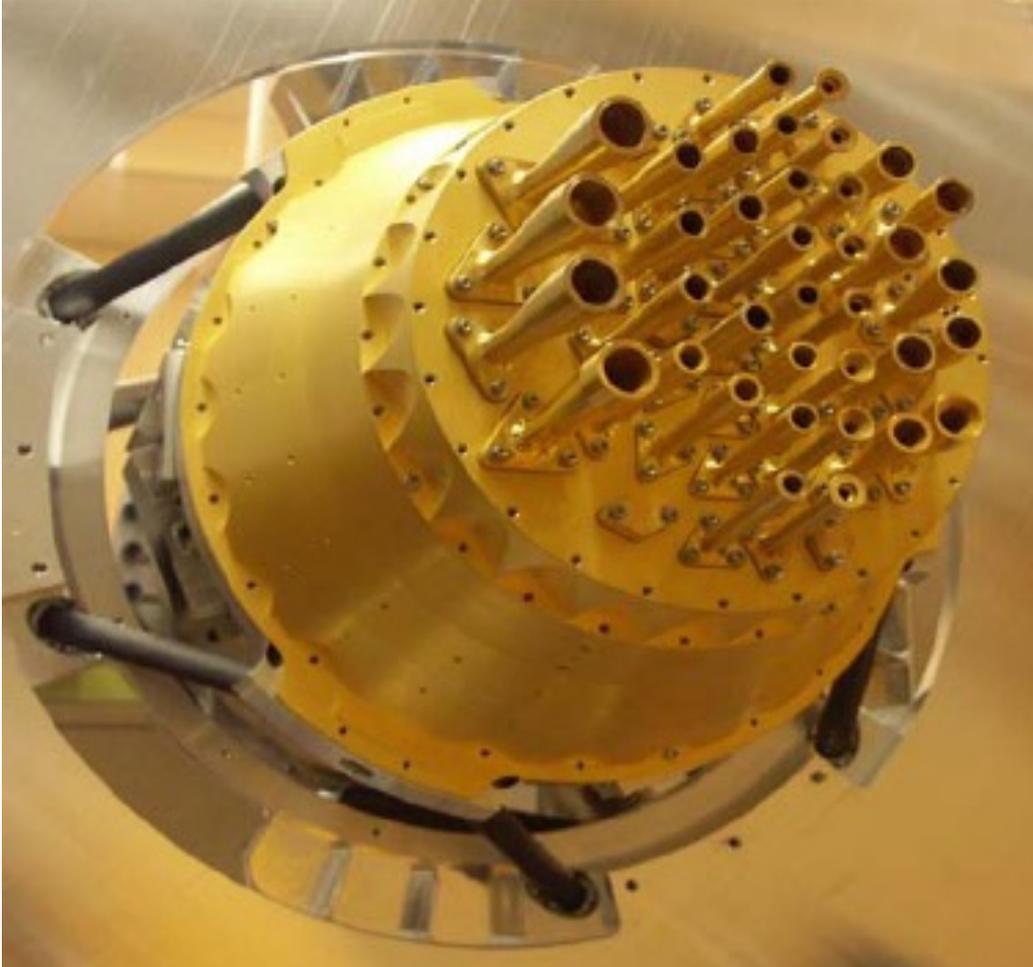
Pour mesurer le fond, on utilise des bolomètres stabilisés à une température de 0.1 K. Leur réchauffement permet de mesurer le rayonnement.

Le fond diffus cosmologique
mesure par le satelllite Planck

Stabilité des bolomètres :
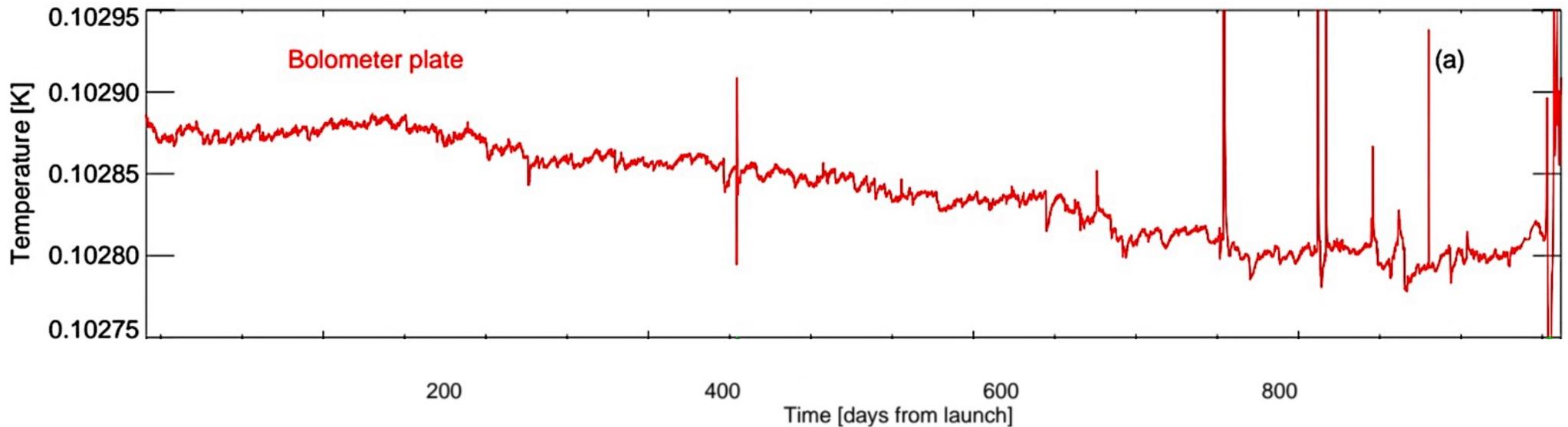
Fig. 7. The impressive stability of the HFI thermal stages during operations. Shown is the temperature evolution of the bolometer stage (*top*), the 1.6 K optical filter stage (*middle*) and the 4-K cooler reference load stage (*bottom*). The horizontal axis displays days since the beginning of the nominal mission.

Individual sources + Radio emission from the Milky Way + Dust emission from the Milky Way + Cosmic Microwave Backgound

All emissions at microwave & submillimetre wavelengths

Le fond diffus cosmologique : image de la plus vieille lumière qui existe, trace fossile de la première lumière qui a pu se propager librement dans l'espace, environ 380 000 ans après le big bang.

recherches récentes

Cryo-electron microscopy of viruses
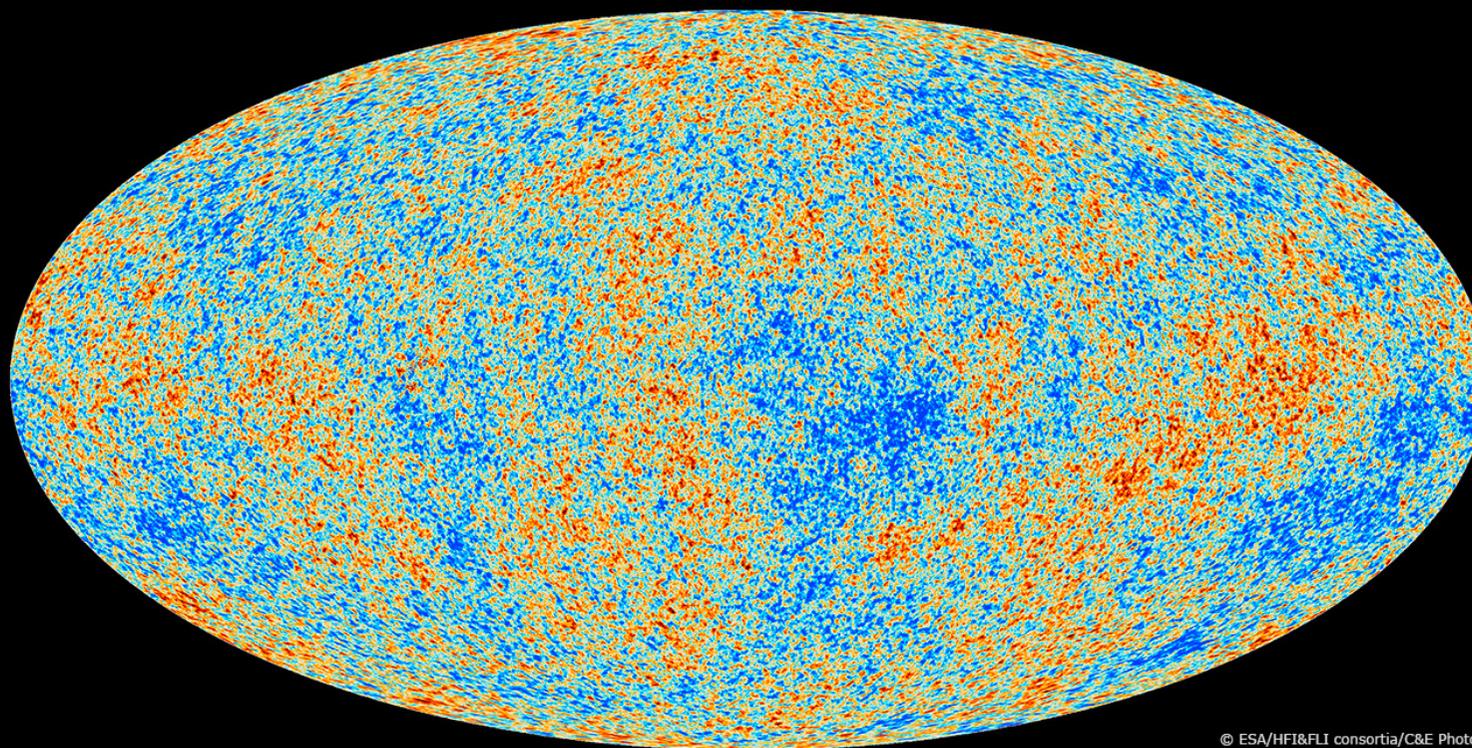
Marc Adrian, Jacques Dubochet, Jean Lepault & Alasdair W. McDowall

European Molecular Biology Laboratory, Postfach 10.2209, D-6900 Heidelberg, FRG

Thin vitrified layers of unfixed, unstained and unsupported virus suspensions can be prepared for observation by cryo-electron microscopy in easily controlled conditions. The viral particles appear free from the kind of damage caused by dehydration, freezing or adsorption to a support that is encountered in preparing biological samples for conventional electron microscopy. Cryo-electron microscopy of vitrified specimens offers possibilities for high resolution observations that compare favourably with any other electron microscopical method.

ALL biological specimens are damaged during preparation for electron microscopy. For particles in suspension, damage is caused by dehydration, adsorption onto the supporting film and by the attempts of the electron microscopist to increase the contrast. Chemical fixation, metal shadowing and negative staining are excellent methods, but they all rely on changing the specimen in order to make it more suitable for observation. As a result electron microscopy has become a highly successful science, but the material observed is generally very different from the original sample.

Cryo-electron microscopy has long been seen as a potential method for preserving the specimen in a state closer to its native state[1]. The value of the approach was demonstrated by Taylor and Glaeser[2], who showed by electron diffraction that the periodic order of frozen-hydrated catalase crystals can be preserved down to less than 3 Å resolution, whereas in air-dried specimens. Another turning point was the discovery that pure water or any aqueous solution can be cooled rapidly enough to prevent formation of ice crystals[3,4]. Based on this phenomenon, we have developed a simple method for preparing and observing frozen-hydrated specimens from native biological suspensions[5-7].
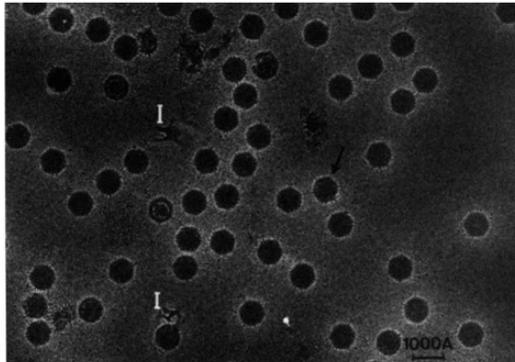
Methodology

The preparation and observation of frozen-hydrated biological particles involved the following operations: (1) forming a thin layer of the suspension; (2) cooling it into the vitreous state; (3) transferring it into the microscope without rewarming above the devitrification temperature ($T_d \cong 140\,K$); and (4) observing it below T_d and with an electron dose low enough to preserve the structure of the specimen.

As discussed below, all these operations are easy to perform and take about the same time as the very simple negative staining procedure. Apart from the requirement for a cooled specimen holder, operating contamination-free below 140 K, there is no need for special instruments or installation.

The formation of a thin layer of aqueous suspension may initially seem difficult, considering the high surface tension of water, which tends to minimize the surface to volume ratio. This difficulty can be overcome, however, when the appropriate surface property is given to the supporting film[5,8,9]. A stable thin layer forms readily in the absence of a supporting film when the liquid is stretched over the holes of a hydrophilic surface. In practice, we put a drop of solution on a clean uncoated 200–600-mesh copper specimen-supporting grid, remove most of the liquid with blotting paper and then freeze. On most specimen grids at least some squares are filled with a film of adequate thickness (<3,000 Å). Better results are obtained if the layer is allowed to become thinner by evaporation while being observed under a low-power microscope. The specimen is frozen after a few seconds, when many grid squares have the right thickness. We refer to this method as the 'bare grid method'. Figure 1 shows a specimen of adenovirus prepared in this way. An alternative way of preparation, referred to as the 'perforated film method', consists of mounting the specimen across the holes of a hydrophilic carbon film. As with the bare

Fig. 1 Thin layer of vitrified suspension of unstained and unfixed adenoviruses type 2, prepared by the bare grid method. A 5-μl drop of suspension containing about 5×10^{11} particles per ml in hypotonic solution was put on a clean uncoated 200-mesh copper grid (Science Services, Münich) pretreated by glow discharge in air[9]. The grid was held by a tweezer mounted on a guillotine and was observed with a stereoscopic microscope at ×20 magnification. Most of the liquid was removed by touching the grid edge with a blotting paper. In the next few seconds, evaporation caused the liquid layer, spread over the grid holes, to break. When about half of the grid holes were still filled, the grid was allowed to fall free from a height of 6 cm into a 1.5-cm deep liquid ethane container, cooled close to solidification temperature by liquid nitrogen. The grid was transferred to liquid nitrogen, mounted in a cold stage PW6591/100 (Philips) and rapidly introduced into a Philips 400 electron microscope where it was kept below 110 K during observation. A dozen grid squares were filled with a layer of adequate thickness. Electron diffraction confirmed that the specimen was vitrified. The micrograph was recorded with 80 kV electrons at ×12,500 magnification, with a total dose of $10\,e\,\text{Å}^{-2}$ and ~8 μm underfocusing. The layer is ~1,200 Å thick. Note the uniform distribution of the viruses and their well defined shape. The superposition of the upper and lower side of the viruses makes the surface structure difficult to interpret. Spikes are visible in favourable cases (arrow). Ice contaminants on the surface are marked (I).

1000Å

Adrian et al., Nature 1984

Heidelberg, Allemagne

1984

une technique de cryogénie pour observer des virus avec un microscope
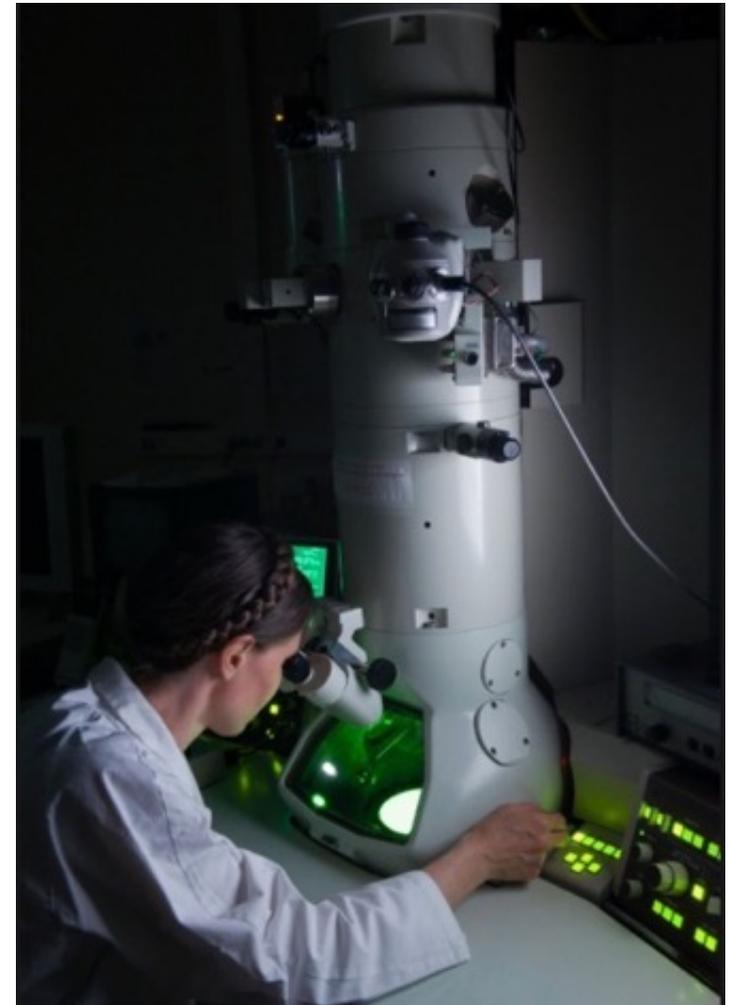
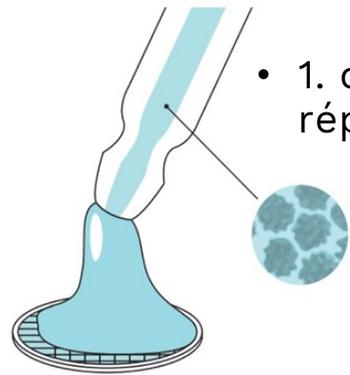# Le froid pour observer la biologie

Le problème :

en microscopie électronique, les électrons détruisent les cellules organiques et brulent tout.

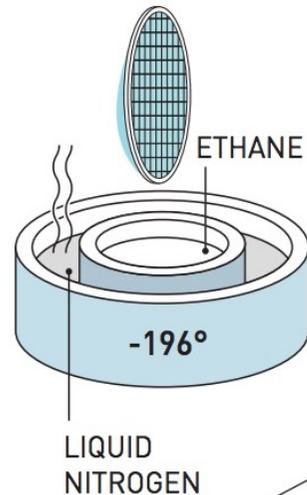Si on protège avec de l'eau, on ne peut plus travailler sous vide.

idée : geler. Mais la glace ordonnée diffuse le faisceau. D'où la technique de vitrification inventée par Dubochet.
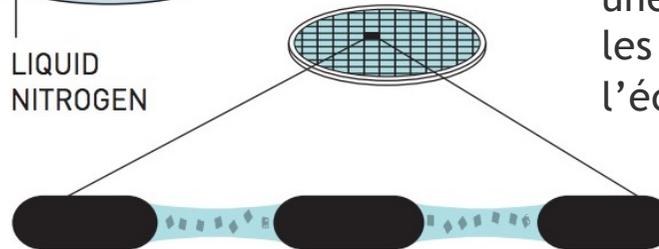
Le froid pour observer la biologie

- 1. on dissout l'échantillon dans l'eau puis on le répartit sur une grille métallique fine

ETHANE

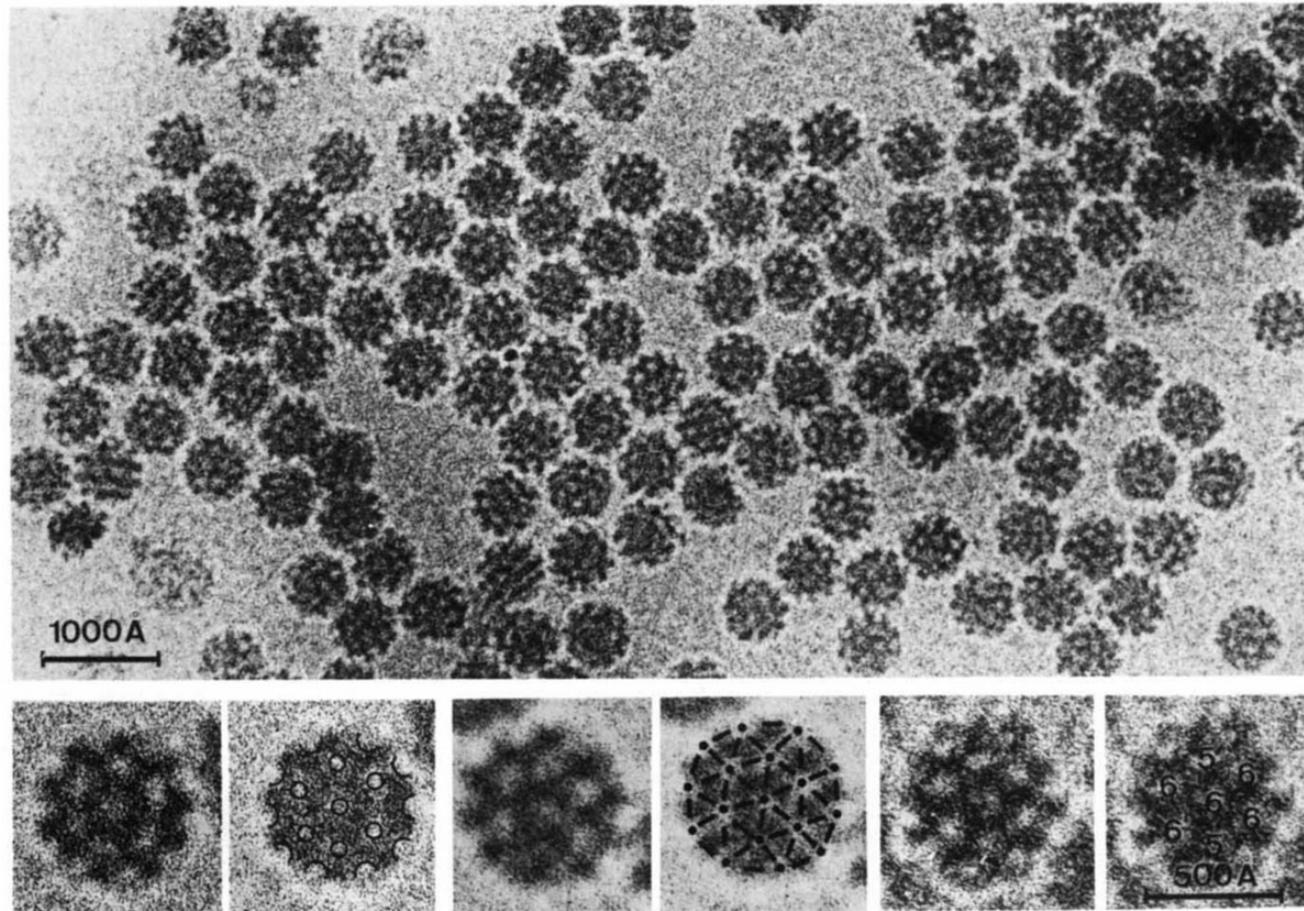2. on plonge dans l'éthane à -190°C entouré d'azote liquide.

-196°

LIQUID NITROGEN

3. l'eau se vitrifie autour de l'échantillon en une structure desordonnée qui ne diffuse plus les électrons. On maintient ensuite froid l'échantillon dans le microscope.

Le froid pour observer la biologie
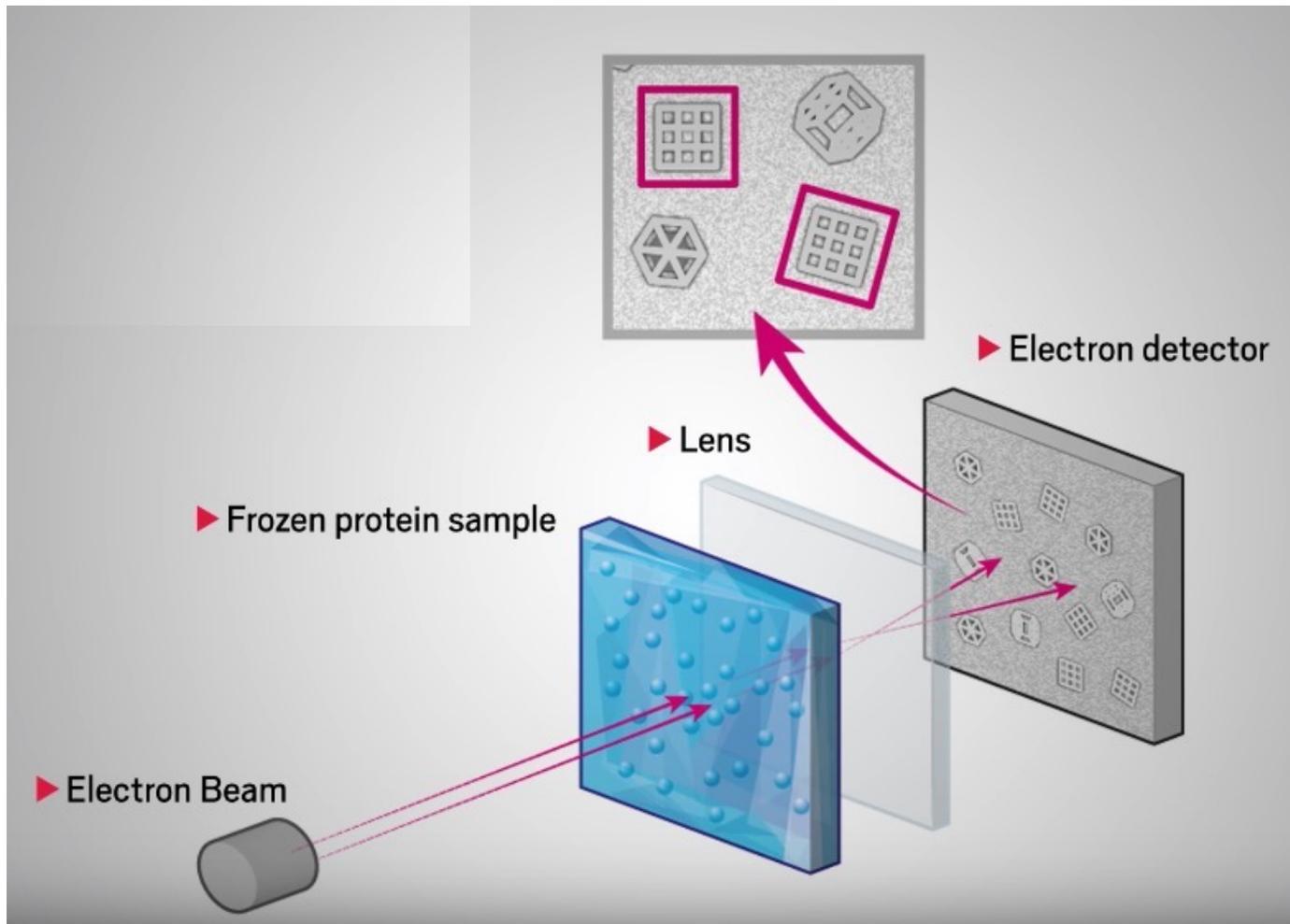
Le froid pour observer la biologie

Premières images de virus

Le froid pour observer la biologie

The Nobel Prize in Chemistry 2017

Jacques Dubochet
Prize share: 1/3

Joachim Frank
Prize share: 1/3

Richard Henderson
Prize share: 1/3

© Nobel Media AB. Photo: A.Mahmoud

The Nobel Prize in Chemistry 2017 was awarded jointly to Jacques Dubochet, Joachim Frank and Richard Henderson "for developing cryo-electron microscopy for the high-resolution structure determination of biomolecules in solution."

La température

Qu'avez-vous retenu ?

La température

Cachez vos notes, et tentez d'écrire en quelques mots...

1 ou 2 ordres de grandeur	un truc que vous avez retenu sur la physique associée	un résultat de recherche récente